IEEE Access
Multidisciplinary | Rapid Review | Open Access Journal

Received 2 April 2023, accepted 16 April 2023, date of publication 24 April 2023, date of current version 4 May 2023.

Digital Object Identifier 10.1109/ACCESS.2023.3269580

RESEARCH ARTICLE

Comprehensive Review of Different Pendulum Structures in Engineering Applications

ZIED BEN HAZEM[1], (Member, IEEE), AND ZAFER BINGÜL[2], (Member, IEEE)
[1]Department of Mechatronics Engineering, College of Engineering (COE), University of Technology Bahrain, Salmabad 18041, Bahrain
[2]Automation and Robotics Laboratory, Department of Mechatronics Engineering, Kocaeli University, 41001 Kocaeli, Turkey

Corresponding author: Zafer Bingül (zaferb@kocaeli.edu.tr)

This work was supported by the University of Technology Bahrain (UTB) under Grant EX610610.

ABSTRACT For years, the pendulum system has been the most popular experimental setup for education and research in robotics and control theory. This paper examines the different kinematic and dynamic structures of pendulum systems, which are frequently used in literature, considering their usage in various engineering fields. Each pendulum system resembles a real physical system and provides a deeper understanding of the behavior of the system. Although each pendulum has its own advantages and disadvantages according to its structure and dynamics, these contain differences depending on the application area and usage method. This paper aims to review and simplify the understanding of the various pendulum systems used in research and applications, presenting a summary of the general properties of pendulum systems to the researcher.

INDEX TERMS Pendulum systems, robotics, control theory and engineering modeling.

I. INTRODUCTION

The inverted pendulum system (IPS) is a benchmark problem for studying nonlinear control design, implementation and development of controllers. It is frequently used in control theory studies and exists in graduate and undergraduate control textbooks as an example of a physical system defined mathematically [1]. IPS is an easily implemented experimental setup to examine and verify the advanced control methods designed for nonlinear systems. The simplified analogous models of IPS are extensively employed in the development of robust balancing control systems for legged humanoid robots, two-wheeled transporters, drones, aerial robots, submarine vessels, satellites, missiles, rockets, etc [2], [3]. The design of robots based on IPS such as legged robots or continuum robots requires fewer actuators for motion control, which results in better control-input efficiency, higher dexterity, and a lesser propensity to break down. High balance control, good trajectory tracking, and robust disturbance rejection are important requirements for these robotics systems in real-time applications. In every control application of IPS, a well-postulated balancing controller is a prerequisite that enables a pendulum to stabilize its posture in a structured environment. The physical analysis of the IPS has been an important consideration in modern control theory studies [4]. Controlling IPS of different configurations is a challenging task but it provides a demonstration model of the capabilities of the natural science and engineering fields [5]. The objective of controlling the IPS is to keep the pendulum in a stable, upward position against the gravitational force by adding a driving force [6], [7]. The pendulum must be stable against the gravitational force, which would make it in an upward position to a more resting-state stable. Different mechanical structures and controllers have been studied to maintain the stability of the IPS. However, the control problem becomes more complicated with additional links and joints [8]. In the literature, many controllers have been used to maintain the inverted pendulum in a stable position. In addition to this purpose, the main control objectives of IPS are stabilization control, swing-up control, and anti-swing control. In this paper, current studies on the control of IPS for different purposes and applications are reviewed in detail. Controller structures can be basically examined as linear and non-linear controllers. Linear controllers used in IPS can be summarized as proportional integral derivative (PID) [9], PI, PD [10], Linear-quadratic regulator (LQR) [11], [102], [103],

The associate editor coordinating the review of this manuscript and approving it for publication was Valentina E. Balas.

linear-quadratic-gaussian (LQG) [103], $\boldsymbol{H_2}$ and $\boldsymbol{H_\infty}$ optimal control [12], etc. The PID controller commonly used in IPS control shows excellent performance due to its robustness in different operation conditions. The linear controllers are easy to implement and very effective in the control of certain IPS but the use of a linearized model can cause instability and poor closed-loop behavior since it cannot fully represent the dynamics of nonlinear systems. Furthermore, the linear controllers are very sensitive the parameter uncertainties and external disturbances in general. The performance of the linear controllers directly depends on the controller parameters and finding optimum parameters for complex nonlinear systems is quite a difficult task. The performance that can be achieved with linear controllers depends on the extent to which the IPS is linear within the operating region. Therefore, the application of linear controllers to the IPS depends on the degree of freedom (DOF) and its complex dynamics. During the past few years, different kinds of non-linear controllers have been applied for IPS control such as nonlinear time-invariant controllers, (sliding mode control (SMC), fuzzy logic control (FLC), [13], [15], [16], self-learning and adaptive nonlinear controllers, model-free controllers [17], neural network (NN) control [14], [20], hybridization of a PID controller and adaptive NN, adaptive NN + PID and adaptive NN + PD controllers [15], [18], [19], etc. FLC, one of the most used nonlinear controller structures, can approximate any nonlinear control law based on the number of fuzzy sets. In the literature, different types of FLC have been developed for different control IPS. Several nonlinear controllers are investigated by researchers to include all nonlinear dynamics of IPS such as full inertia tensor, linear and non-linear friction models, etc. Nonlinear control methods take advantage of the given accurate model of nonlinear system dynamics to achieve high-performance control. No linearization or gain scheduling is needed for their implementation. Also, the stability of the resulting system can be tested with the Lyapunov stability theory. The control of the IPS typically relies on accurate dynamic models and the parameters of the controller are optimally calculated from this model. Recent literature on this topic addresses control approaches for a variety of systems having common explicit dynamic models in the control loop. Therefore, the dynamic parameters of IPS are a key topic for advanced nonlinear control design, where all physical variables need to be taken into account. Like the correct inertial tensors to consider, the dynamic parameters of the IPS need to be found with precision. In this paper, to examine the effects of the inertia of the pendulums, the dynamic equations of the triple link rotary inverted pendulum are solved in three different inertia cases: In the first case, the inertia matrix of the links is neglected in the dynamic model. In the second case, only component z of the inertia matrix is considered. In the last case, the full inertia matrix is taken into consideration in the dynamic model. The results of the dynamic equations with only the component z of the inertia matrix and the full inertia matrix are almost the same in low and medium velocities but not the same for higher velocities. The accurate dynamic model in the nonlinear control design of the IPS is very important for this reason the full inertia must be taken into consideration in the dynamic model of IPS with a complex structure. Most of the controller structures require knowledge of the dynamic model of the systems, and their control performance is highly dependent on obtaining the optimum parameter of the controller directly depending on the accuracy of the dynamic model in real-world applications. The assumptions in the current literature that links, and their joints are massless and without inertial do not fully reflect the behavior of real-world pendulum systems. Therefore, the effects of mass and inertia need to be considered to obtain more realistic results. This study is aimed to examine the effects of mass and inertia on the dynamic equations of motion of pendulum systems. The advantages of this work are to examine the different kinematic and dynamic structures of IPS which are frequently used in literature. The main contribution of this study is the necessity of using an accurate dynamic model (full inertia matrix and nonlinear friction models) of IPS with complex dynamics for nonlinear control. Furthermore, there is no advantage in using approximate parameters of the dynamic model because it can conduct a poor performance in the nonlinear control due to the complex and coupled dynamics of the IPS. Dynamic modeling of IPS has been extensively studied using general approaches, however, it is difficult to obtain a dynamic model using all physical variables. Therefore, most control applications use very simplified models instead of finding the correct dynamic parameter. Modeling the nonlinear dynamic effects of friction, actuator characteristics, and inertia tensors could pose challenges in the parameter identification of the IPSs. These are examples of areas where further research and development work are needed. A simple model of the IPS, consisting of a pendulum link attached directly to the shaft of a motor, is shown in Figure 1. A classification of IPS based on the number of actuators is given in Figure 2. In this paper, the different kinematic and dynamic structures of pendulum systems frequently used in research and engineering are explored and analyzed. The paper provides an overview of the ways in which these systems can be used to gain insight into the behavior of real-life physical structures. The dynamic complexity of each pendulum system is discussed, including the pros and cons of each system depending on the field of application. The paper presents typical applications of each pendulum system and provides a comprehensive review of the existing control strategies for pendulum systems in robotic research. The aim of this paper is to provide a comprehensive review of the pendulum systems and the control strategies used for their control. It begins by examining different kinematic and dynamic structures of the pendulum systems used in engineering, which resemble real-life physical systems. The advantages and disadvantages of each pendulum system are discussed based on the field of application and usage. The paper then moves on to the modeling of the IPS and provides an overview of the various control strategies used for its control. The challenges and trends in the field are also

discussed. The paper concludes by summarizing the findings and offering insights into future research directions.

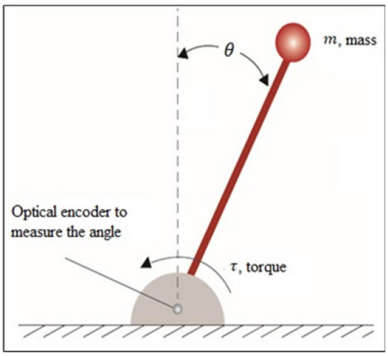

FIGURE 1. A simple model of the IPS.

II. PENDULUM SYSTEM TYPES: AN OVERVIEW

Different types of pendulum systems are used in various industrial sectors. Generally, these pendulum systems may be categorized into two groups, based on their structures and number of actuators: (1) single-actuator pendulum systems, and (2) multi-actuator pendulum systems. The single-actuator pendulum systems have a single actuator that provides the control input to the system. The actuator may be either a motor or a hydraulic system. The inverted pendulum system (IPS) is the most common single-actuator pendulum system and is used as an example in undergraduate control textbooks. The objective of controlling the IPS is to maintain the hinged pendulum in a stable position, usually upward, by adding a driving force. Multi-actuator pendulum systems, on the other hand, have more than one actuator, which provides control inputs to the system. The control problem becomes more complicated with the addition of more actuators, but the pendulum system can be more flexible and responsive to external disturbances. These systems are used in various applications, including advanced robotics and mechatronic systems. The classification of the IPS according to the actuator configuration is illustrated in Figure 2.

A. SINGLE ACTUATOR LINEAR SERIAL IPS

1) SINGLE ACTUATOR LINEAR SERIAL IPS

In summary, Figure 3 illustrates the kinematics representation and a real experimental implementation of the SLLIP, where a motor is used to move a cart linearly along a straight track to modify the pendulum angle. The SLLIP has two equilibrium points, one in the upward vertical position above the cart and the other similar to the gantry crane system control. The objective of the control of the SLLIP is to maintain the pendulum in the upward vertical position and prevent it from falling [21], [22]. [23].

2) DOUBLE LINK LINEAR INVERTED PENDULUM (DLLIP)

Figure 4 demonstrates the kinematic representation and a real-world implementation example of a DLLIP (Double Link Inverted Pendulum). The DLLIP is an extension of the SLLIP (Single Link Inverted Pendulum) by adding another vertical pendulum link. The DLLIP has a cart that can move linearly and two pendulum links connected in series to the cart. It has two equilibrium points, one being the maintenance of the two pendulums in an upward vertical position above the cart, which is mostly used to study the control of humanoid robots. The second equilibrium point is maintaining the two pendulums in an up-down vertical position, which is similar to the problem of controlling a crane system with a double pulley [24], [25], [26].

3) TRIPLE LINK LINEAR INVERTED PENDULUM (TLLIP)

A kinematics representation and a real experimental example of the TLLIP system are shown in Figure 5. TLLIP is the extension of the DLLIP by another vertical pendulum link. The TLLIP has two equilibrium points, which are used to analyze the control problem of different engineering systems. The first equilibrium problem of this system consists of maintaining the three pendulums in the upward vertical position above the cart. The first equilibrium problem is mostly used to analyze the control of humanoid robots. From the bottom of the foot to the top of the leg, present the first pendulum. From the top of the leg to the bottom of the neck represents a second pendulum. A third pendulum represents a neck with the head of a human. The second equilibrium problem consists of maintaining the three pendulums in the up-down vertical position and is similar to the control problem of the crane system with more than double pulley, each wire rope and pulley present a pendulum [27], [28], [29], [30], [31].

- In summary, the IPSs are pendulum systems that can be categorized into single-actuator and multi-actuator systems based on their structures and the number of actuators. Examples of single-actuator systems include the SLLIP, which has two equilibrium points at the up and down positions and is used to analyze control problems in space rockets and human-mounted bicycles. Examples of multi-actuator systems include the DLLIP and TLLIP, which are extensions of the SLLIP with additional pendulum links. These systems are used to analyze the control of humanoid robots and crane systems with multiple pulleys.

4) LINEAR FLEXIBLE INVERTED PENDULUM (LFIP)

Figure 6 shows a kinematics representation of a LFIP. LFIP is composed of a flexible pendulum link that moves horizontally by the cart and a load is attached at the end of the pendulum link. The main objective of this IPS model according to the other IPS modes is to take into consideration the large deformations of the pendulum link; its length is assumed constant, cause to a holonomic constraint. The LFIP can be used to analyze the control problem of biomedical engineering systems such as the flex-foot cheetah prosthetic. The prosthetic is flexibly used to maintain the disabled human in the vertical equilibrium position. The dynamic model of the prosthetic presents an LFIP and the human leg presents the loaded mass to the prosthetic [32], [33].

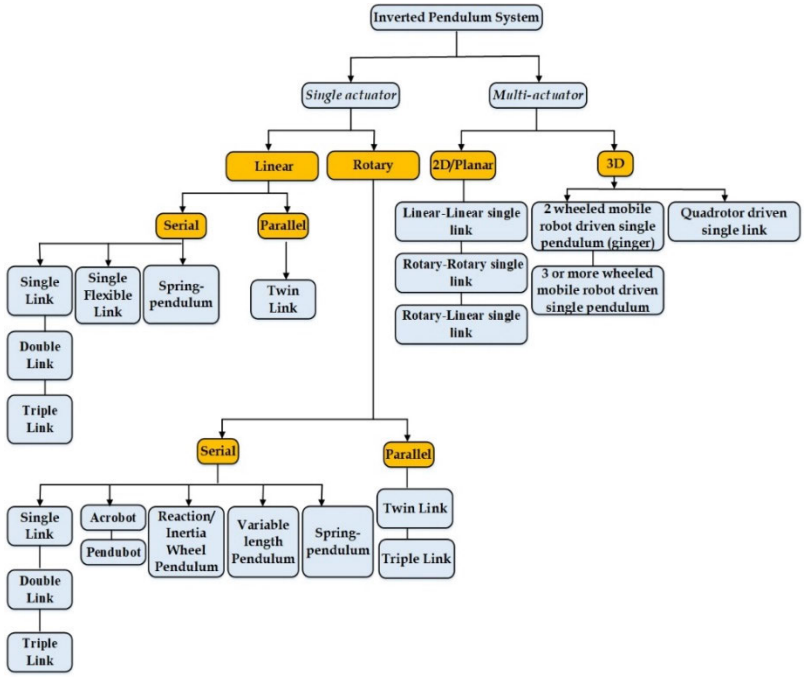

FIGURE 2. Classification of the IPS according to the actuator configuration.

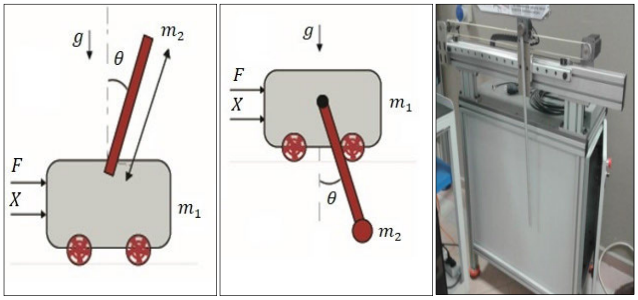

(a) (b) (c)

FIGURE 3. SLLIP: (a) Kinematics representation of a cart-pole system, (b) Kinematics representation of a crane system, and (c) real experimental implementation.

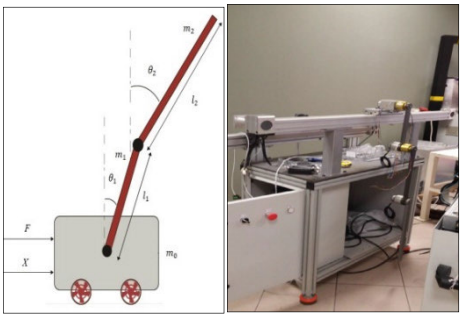

(a) (b)

FIGURE 4. DLLIP: (a) Kinematics representation and (b) real experimental implementation.

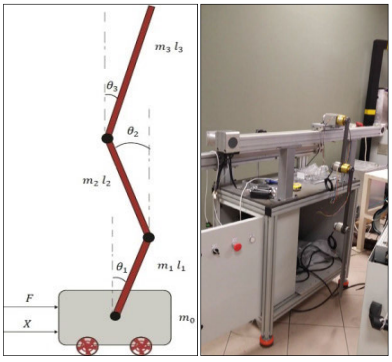

(a) (b)

FIGURE 5. TLLIP: (a) Kinematics representation and (b) real experimental implementation.

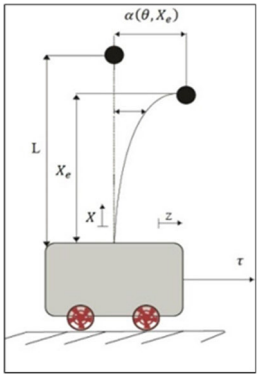

FIGURE 6. Kinematics representation of the LFIP.

5) SPRING-LOADED INVERTED PENDULUM (SLIP)

Figure 7 shows the kinematics representation of the SLIP system, which consists of a point mass attached to a massless leg with a linear spring. The SLIP model is used to analyze the run and hop of different species and contains flight and stance phases. The flight phase involves a ballistic path of the point mass until the foot contacts the soil surface at a fixed angle,

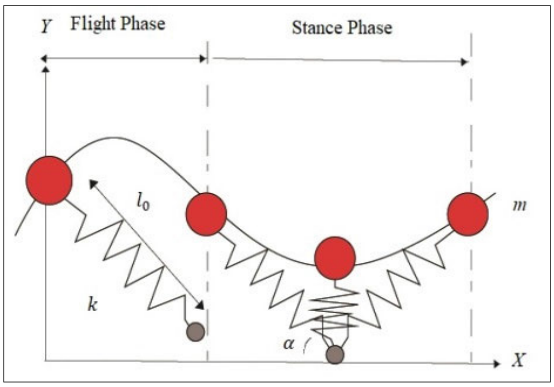

FIGURE 7. Kinematics representation of the standard SLIP.

marking the start of the stance phase where the position of the foot stays fixed, the spring compresses, and the point mass moves. When the lengths of the spring and the resting spring are equal, the spring flies away and the flight phase restarts. The SLIP model was introduced by Blickhan and is widely used in the study of legged locomotion [34], [35], [36].

6) VARIABLE LENGTH INVERTED PENDULUM (VLIP)

Figure 8 (a) depicts a kinematics representation of the VLIP system, which is composed of a pendulum link that moves in a vertical position and a sliding mass attached to the variable pendulum link length. The system's objective is to maintain the pendulum link in a vertical position while changing the sliding mass position. Figure 8 (b) shows a kinematic representation of a double pendulum with a variable length (DPVL), which provides a simplified and accurate model for planning static and dynamic human-like robots. Both the static and motion dynamics of human postures can be described with the variable parameters of the DPVL [37], [38], [39].

B. SINGLE ACTUATOR LINEAR PARALLEL IPS

1) LINEAR TWIN INVERTED PENDULUM (LTIP)

A kinematics representation of the LTIP is shown in Figure 9. The LTIP system is a representation of biped walking robots where two parallel pendulum links are mounted on a cart moving on a rail. The aim is to maintain the two pendulum links in an upward vertical position. The LTIP can be used to analyze the control problem of a biped walking robot and the dynamics of a biped walking robot can be modeled by the two parallel-inverted pendulums of the LTIP system [40], [41], [42].

- In summary, the various IPS models (LFIP, SLIP, VLIP, LTIP, and SLRIP) are used in the analysis and control of different engineering systems such as biomedical systems, legged locomotion, biped robots, mobile robots, flexible-link robots, rotary crane systems, etc. Each IPS model has its own unique structure and dynamics and is used to study the control problems in a particular system by taking into account the relevant physical characteristics and constraints of that system.

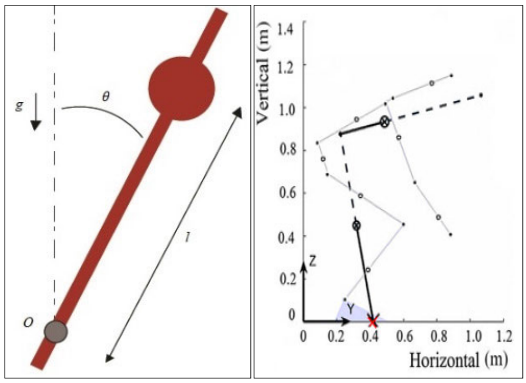

FIGURE 8. Kinematics representation of (a) VLIP and (b) DPVL [39].

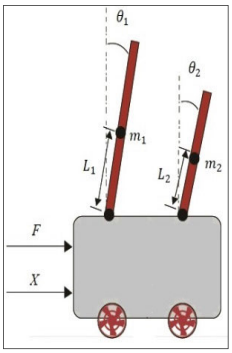

FIGURE 9. Kinematics representation of the LTIP.

C. SINGLE ACTUATOR ROTARY IPS

1) SINGLE LINK ROTARY INVERTED PENDULUM (SLRIP)

Figure 10 shows a kinematics representation and real experimental implementation examples of a SLRIP. The SLRIP is composed of a pendulum link mounted to the horizontal arm via a joint. The rotation axis of the pendulum link is collinear with the axis of the horizontal arm link. The horizontal arm link is coupled directly to the motor shaft giving it rotary motion. The system input is the torque applied by the motor. The SLRIP system is called the "Furuta Pendulum" [43]. The SLRIP has two equilibrium problems used in the control analysis of different engineering systems. The first equilibrium problem consists of maintaining the pendulum in the upward vertical position above the cart. This equilibrium problem is mostly used to analyze the control of include walking robots, mobile robots, flexible-link robots, robots on mobile platforms, etc. The second equilibrium problem consists of maintaining the pendulum in the up-down vertical position in the control problem of the rotary crane system [34], [35], [36].

2) DOUBLE AND TRIPLE LINK ROTARY INVERTED PENDULUM (DLRIP/TLRIP)

The DLRIP and TLRIP are shown in Figures 11 (a) and (b), respectively. The DLRIP and TLRIP are models used in the control analysis of engineering systems such as robots and cranes. The DLRIP consists of two serial pendulum links of different lengths attached to an extremity of a horizontal arm, with a torque servo motor in the middle supplying the torque

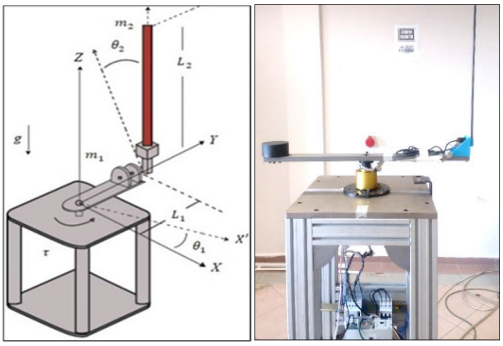

FIGURE 10. SLRIP: (a) kinematics representation and (b) real experimental implementation.

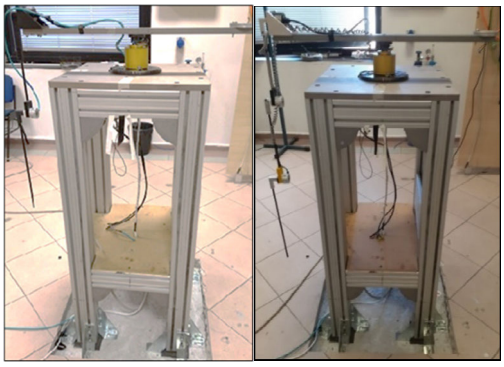

FIGURE 11. (a) DLRIP and (b) TLRIP.

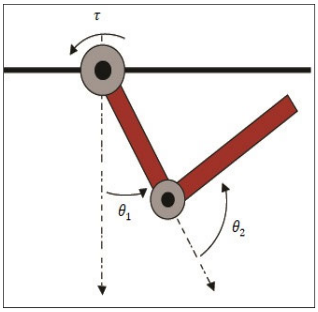

FIGURE 12. Kinematics representation of the Pendubot.

input. The TLRIP is an extension of the DLRIP with an additional vertical pendulum link, consisting of a horizontal arm and three serial pendulum links. The angles of the pendulum links in both systems, DLRIP and TLRIP, are represented by is $\theta_1\theta_1$, θ_2, θ_3 and θ_4. These models are used to analyze the control and dynamics of different systems [47], [48].

3) PENDUBOT

The Pendubot is used in the study of control problems in mechanical engineering, specifically in the analysis of the stability and control of multi-link systems. The system is useful in the design and control of flexible robots, mobile robots, and rotary crane systems. The angles of the pendulum links can be controlled by torque motors, and the goal of control is to maintain the system at the equilibrium points, making it a useful tool for the study of dynamic control problems [49], [50], [51]. The kinematics representation of a Pendubot is shown in Figure 12.

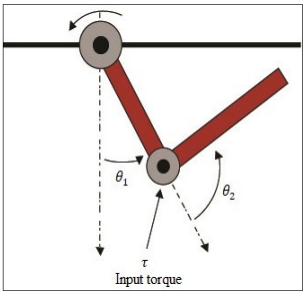

FIGURE 13. Kinematics representation of the Acrobot.

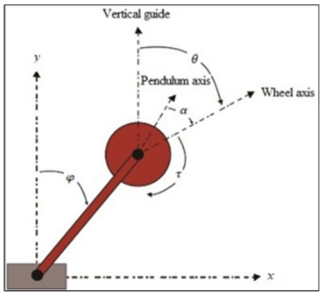

FIGURE 14. Kinematics representation of the RWP.

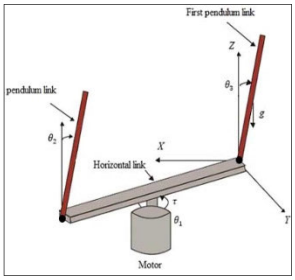

FIGURE 15. Kinematics representation of the RTIP.

4) ACROBOT

Acrobot system is also used to study energy-based control strategies, where the control input is used to conserve or transfer energy between the system's kinetic and potential energy. This type of control can lead to more efficient and robust control in comparison to traditional position-based control [54]. The Acrobot system can be considered a good testbed for exploring and testing different control methods in robotics [52], [53]. Figure 13 shows examples of a kinematics representation of an Acrobot system.

5) A REACTION WHEEL PENDULUM (RWP)

The RWP system is widely used to study the control problems in various engineering systems, such as self-balancing unicycle, segway, and other balancing systems. The torque input from the servo motor allows the system to be controlled and balanced, which is critical in these types of applications. Understanding the dynamics and control problems of the RWP system is crucial for the development and design of

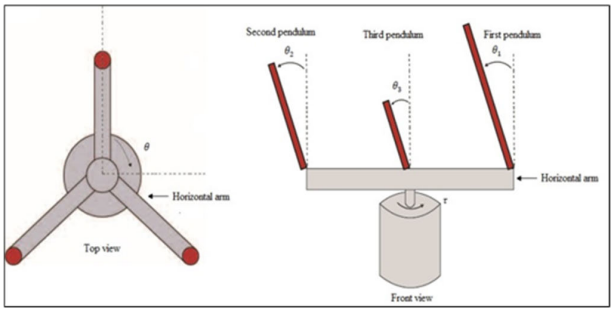

FIGURE 16. Kinematics representation of the RTIP.

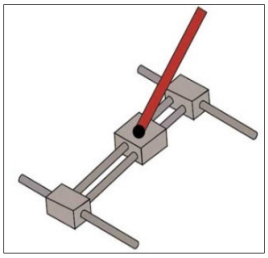

FIGURE 17. Kinematics representation of the LLPIP.

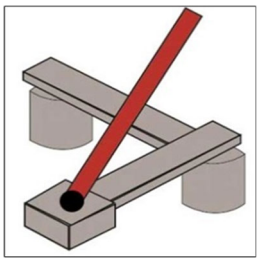

FIGURE 18. Kinematics representation of a RRPIP.

these systems [54], [55]. The kinematics representation of the RWP system is depicted in Figure 14.

6) ROTARY TWIN INVERTED PENDULUM (RTIP)

A kinematics representation of RTIP is shown in Figure 15. The RTIP system is mainly used to study the control of multi-pendulum systems and is also applied to the control analysis of complex engineering systems such as flexible-link robots and multi-link robots. The RTIP can also be used to analyze the control problem of amusement park rides such as the rotor ride [56], [13].

7) ROTARY TWIN INVERTED PENDULUM (RTIP)

The RTLIP is a complex system that aims to stabilize three pendulum links in an upward position through the use of three rotary horizontal arms and a servomotor. The kinematic representation of the RTLIP is shown in Figure 16. The RTLIP has six parts and the dynamics of the system are similar to the motion of two or more humans in a rotor ride [13], [57].

D. MULTI-ACTUATOR PLANAR IPS

1) LINEAR-LINEAR PLANAR INVERTED PENDULUM (LLPIP)

The LLPIP system is widely used to study dynamic balance control and stabilization problems in various applications, such as biped robots, quadruped robots, mobile robots, and

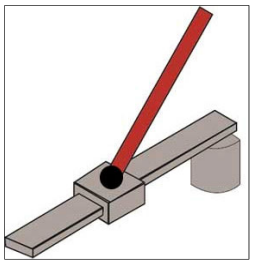

FIGURE 19. Kinematics representation of a RLPIP.

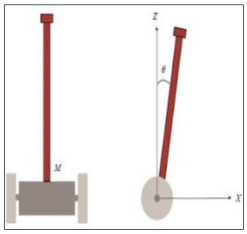

FIGURE 20. Kinematics representation of the TWIPMR.

aerial robots [59], [60], [61]. The complexity of the PIP system lies in its two DOF configurations, which makes the system more challenging to control compared to single DOF systems like the IPS, RTIP, and RTLIP. However, the LLPIP system also has a higher degree of freedom, which makes it more versatile and adaptable to different scenarios [58]. The kinematics representation of a LLPIP is shown in Figure 17.

2) ROTARY-ROTARY PLANAR INVERTED PENDULUM (RRPIP)

A kinematics representation of a RRPIP is shown in Figure 18. The control problem of the RRPIP involves stabilizing the pendulum link in the upward position by controlling the torque applied by the servo motor at the joint. The RRPIP presents a more complex control problem compared to the LLPIP and is used to study the dynamics of a satellite during orbit [59].

3) ROTARY-LINEAR PLANAR INVERTED PENDULUM (RLPIP)

The kinematics representation of a RLPIP is shown in Figure 19. The RLPIP system aims to stabilize the pendulum link in the upward vertical position by controlling the rotational and linear inputs. The interaction of the rotational and linear inputs makes the RLPIP a complex system compared to the other types of inverted pendulum systems [60].

E. MULTI-ACTUATOR 3D IPS

1) TWO-WHEELED INVERTED PENDULUM MOBILE ROBOT (TWIPMR)

The kinematics representation of a TWIPMR (Two-Wheeled Inverted Pendulum Mobile Robot) is shown in Figure 20. TWIPMR is based on the concept of an Inverted Pendulum System (IPS) and is used for tasks such as service robots, human transportation, and baggage transportation, among others. TWIPMR can balance with two wheels and make sharp turns. It is inherently unstable, but by driving the motors in the right direction, the system returns to a stable, upright

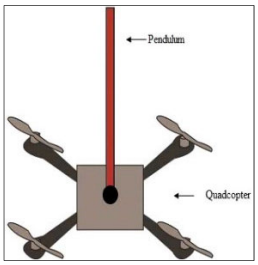

FIGURE 21. Kinematics representation of the QDIP.

position. The two wheels are the only two points of contact with the ground. The aim is to balance the pendulum at zero degrees ($\theta = 0°$). Additionally, this system can be driven with multiple wheels, and such a configuration is called a Multi-Wheeled Inverted Pendulum Mobile Robot (MWIPMR) [61], [62], [63], [64].

2) QUADROTOR DRIVEN INVERTED PENDULUM (QDIP)

The kinematics representation of a QDIP is shown in Figure 21. The QDIP system has two main components: the quadrotor and the inverted pendulum link. The quadrotor provides the necessary lift and control to stabilize the pendulum link, which is mounted on the top of the quadrotor. The goal of the control system is to keep the pendulum link in the upward vertical position, which is an inherently unstable configuration. This system is used to study the dynamics of a human in a fly-board air system, where the human acts as the inverted pendulum and the fly-board as the quadrotor [66], [67].

III. PENDULUM SYSTEM: MODELING

The serial IPS can be considered an under-actuated system. The kinematics equations of the IPS may be obtained based on the Denavit-Hartenberg method. ${}^{i-1}_{i}T$ is the homogeneous transformation matrix from the coordinate attached to an $i^{-\text{th}}$ link to a coordinate attached to $\mathrm{i}^{-1-\text{th}}$ link, $i = 1 \ldots n$, can be given as follows:

$$
{}^{i-1}_{i}T = \begin{bmatrix} \cos\theta_i & -\sin\theta_i & 0 & a_{i-1} \\ \sin\theta_i \cos a_{i-1} & \cos\theta_i \cos a_{i-1} & -\sin a_{i-1} & -\sin a_{i-1} d_i \\ \sin\theta_i \sin a_{i-1} & \cos\theta_i \sin a_{i-1} & \cos a_{i-1} & \cos a_{i-1} d_i \\ 0 & 0 & 0 & 1 \end{bmatrix} \tag{1}
$$

Rotation and homogeneous transformation matrices between coordinates of the serial IPS can be calculated. The nonlinear motion equations of serial IPS are derived based on the DH convention. Furthermore, the nonlinear equations of the serial IPS are derived based on the "Euler-Lagrangian" method using rotation and homogeneous transformation matrices [68], [69]. The nonlinear equations of the IPS are given in equation (2):

$$
D(\theta)\ddot{\theta} + C\left(\theta, \dot{\theta}\right) + G(\theta) = \begin{bmatrix} \tau_1 \\ 0 \\ 0 \end{bmatrix} \tag{2}
$$

TABLE 1. Parameters and variables of the system.

Symbol	Description	Unit
θ_i	Angle of i-th link.	[rad]
τ_i	Torque for the i-th link.	[Nm]
I_1	Inertia tensor of i-th link.	[kg m^2]
I_{zzi}	Z-component of the inertia tensor of i-th link.	[Kg m^2]
m_i	Mass of i-th link.	[kg]
m_B	Mass of balance mass.	[kg]
L_i	Length of i-th link.	[m]
b_i	Viscous damping coefficient of i-th link.	[N-m-s/rad]
g	Gravity	[N kg^{-1}]

where the vector of joint positions is θ, the vectors of angular velocities is $\dot{\theta}$, and the vector of angular accelerations is $\ddot{\theta}$. $D(\theta)$, $C\left(\theta, \dot{\theta}\right)$, $G(\theta)$ and τ_1 are mass matrix, vector of centrifugal and Coriolis forces, gravity force vector, and torque input in θ_1. The terms of the mass matrix are calculated using equation (3).

$$
D(\theta) = \sum_{i=1}^{n} \left[(A_i)^T m_i A_i + (B_i)^T I_i B_i \right] \tag{3}
$$

$\mathrm{m_i}$ is the mass of $\mathrm{i^{th}}$ link; $\mathrm{I_i} \in \mathrm{R3 \times 3}$ is the inertia tensor in the mass center of the $\mathrm{i^{th}}$ link. $\mathrm{A_i}$ and $\mathrm{B_i} \in \mathrm{R\ 3\times\ n}$ are Jacobian matrices. The terms of Coriolis and Centripetal vector are calculated using the equations as follows, [66]:

$$
C\left(\theta, \dot{\theta}\right) = \sum_{k=1}^{n} \sum_{j=1}^{n} \left[c^{i}_{kj}(\theta)\, \dot{\theta}_k \dot{\theta}_j \right] \tag{4}
$$

$$
\mathrm{c^{i}_{kj}}(\theta) = \frac{\partial}{\partial \theta_{\mathrm{k}}} \mathrm{D_{ij}}(\theta) - \frac{1}{2} \frac{\partial}{\partial \theta_{\mathrm{i}}} \mathrm{D_{kj}}, \quad 1 \leq \mathrm{i, j, k} \leq \mathrm{n} \tag{5}
$$

The gravity vectors can be calculated using equation (6).

$$
\mathrm{G}(\theta) = -\sum_{\mathrm{k=1}}^{\mathrm{n}} \sum_{\mathrm{j=1}}^{\mathrm{n}} \left[\mathrm{g_k m_j A^{j}_{ki}}(\theta) \right] \tag{6}
$$

A. MODELING OF THE SLRIP

The SLRIP is assumed to be a serial kinematic chain. The kinematic model of the system is derived based on the DH convention. Rotation and homogeneous transformation matrices between coordinates of the SLRIP are calculated. The parameters and variables of all models are given in Table 1. DH Parameters of the SLRIP are given in Table 2. The homogeneous transformation matrix of the SLRIP is derived in equation (7), as shown at the bottom of the next page, using the DH parameters in Table 2.

The dynamic equations of the SLRIP are derived in the matrix form in equation (8), as shown at the bottom of the next page.

B. MODELING OF THE DLRIP

The DLRIP is assumed to be a serial kinematic chain, it is the extension of SLRIP. DH Parameters of the DLRIP are given in Table 3. The homogeneous transformation matrix of

TABLE 2. DH-parameters of the SLRIP.

Coordinate	A_{i-1}	a_{i-1}	d_i	θ_i
1	0	0	0	θ_1
2	$-\frac{\pi}{2}$	0	L_1	$\theta_2-\frac{\pi}{2}$
3	0	L_2	0	0

TABLE 3. DH-parameters of the DLRIP.

Coordinate	A_{i-1}	a_{i-1}	d_i	θ_i
1	0	0	0	θ_1
2	$-\frac{\pi}{2}$	0	L_1	$\theta_2-\frac{\pi}{2}$
3	0	L_2	0	θ_3
4	0	L_3	0	0

the DLRIP is derived in equation (9). Simplified parameters description of the DLRIP are given in Table 5, see appendix.

$$
\begin{aligned}
{}^0_4\mathrm{T} &= {}^0_1\mathrm{T}\,{}^1_2\mathrm{T}\,{}^2_3\mathrm{T}\,{}^3_4\mathrm{T} \\
&= \begin{bmatrix}
\sin\theta_{23}\cos\theta_1 & \cos\theta_{23}\cos\theta_1\ldots & -\sin\theta_1 & \mathrm{L}_2\cos\theta_1\sin\theta_2-\mathrm{L}_1\sin\theta_1 \\
\sin\theta_{23}\sin\theta_1 & \cos\theta_{23}\sin\theta_1\ldots & \cos\theta_1 & \mathrm{L}_1\cos\theta_1+\sin\theta_1(\mathrm{L}_3\sin\theta_{23}+\mathrm{L}_2\sin\theta_2) \\
\cos\theta_{23} & -\sin\theta_{23}\ldots & 0 & \mathrm{L}_3\cos\theta_{23}+\mathrm{L}_2\cos\theta_2 \\
0 & 0\ldots & 0 & 1
\end{bmatrix}
\end{aligned} \tag{9}
$$

where $\theta_{23}=\theta_2+\theta_3$.

The expression of the mass matrix of the DLRIP is given in equation (10)

$$
\mathrm{D}(\theta)=\begin{bmatrix}\mathrm{D}_{11} & \mathrm{D}_{12} & \mathrm{D}_{13}\\ \mathrm{D}_{21} & \mathrm{D}_{22} & \mathrm{D}_{23}\\ \mathrm{D}_{31} & \mathrm{D}_{32} & \mathrm{D}_{33}\end{bmatrix} \tag{10}
$$

The elements of the mass matrix of the DLRIP system are given as follows:

$$
\begin{aligned}
\mathrm{D}_{11} &= \mathrm{I}_{zz_1}+\frac{\mathrm{I}_{zz3}}{2}+\mathrm{a}_6+\frac{\mathrm{a}_4}{2}+\frac{\mathrm{a}_7}{8}-\frac{\mathrm{I}_{zz3}\cos(2\theta_2+2\theta_3)}{2} \\
&\quad -\frac{\mathrm{a}_7\cos(2\theta_2+2\theta_3)}{8}\frac{\mathrm{a}_8\cos(\theta_3)}{2} \\
&\quad -\frac{\mathrm{a}_8\cos(2\theta_2+\theta_3)}{2}+\frac{\mathrm{a}_3}{4} \\
&\quad +\left(\frac{\mathrm{a}_2\sin^2\theta_2}{4}+\mathrm{a}_5\right)-\frac{\mathrm{a}_4\cos(2\theta_2)}{2}
\end{aligned} \tag{11}
$$

$$
\mathrm{D}_{12}=-\frac{\mathrm{a}_{11}\cos(\theta_2+\theta_3)+2\mathrm{a}_{10}\cos\theta_2}{2}+-\left(\frac{\mathrm{a}_9\cos\theta_2}{2}\right) \tag{12}
$$

$$
\mathrm{D}_{13}=-\frac{\mathrm{a}_{11}\cos(\theta_2+\theta_3)}{2} \tag{13}
$$

$$
\mathrm{D}_{22}=\mathrm{a}_4+\mathrm{a}_8\cos\theta_3+\frac{\mathrm{a}_1}{4}+\mathrm{I}_{zz3}+\left(\frac{\mathrm{a}_2}{4}+\mathrm{I}_{zz_2}\right) \tag{14}
$$

$$
\mathrm{D}_{23}=\frac{\mathrm{a}_1}{4}+\frac{\mathrm{a}_8\cos\theta_3}{2}+\mathrm{I}_{zz3} \tag{15}
$$

$$
\mathrm{D}_{33}=\frac{\mathrm{a}_7}{4}+\mathrm{I}_{zz3} \tag{16}
$$

$$
\mathrm{D}_{21}=\mathrm{D}_{12},\quad \mathrm{D}_{31}=\mathrm{D}_{13} \tag{17}
$$

The expression of the Coriolis and Centripetal force vector is given in equation (18)

$$
\mathrm{C}\left(\theta,\dot{\theta}\right)=\begin{bmatrix}\mathrm{C}_{11}\\ \mathrm{C}_{21}\\ \mathrm{C}_{31}\end{bmatrix} \tag{18}
$$

$$
{}^0_3\mathrm{T}={}^0_1\mathrm{T}\,{}^1_2\mathrm{T}\,{}^2_3\mathrm{T}=\begin{bmatrix}\sin\theta_2\cos\theta_1 & \cos\theta_2\cos\theta_1 & -\sin\theta_1 & \mathrm{L}_2\cos\theta_1\sin\theta_2-\mathrm{L}_1\sin\theta_1\\ \sin\theta_2\sin\theta_1 & \cos\theta_2\sin\theta_1 & \cos\theta_1 & \mathrm{L}_1\cos\theta_1+\mathrm{L}_2\sin\theta_1\sin\theta_2\\ \cos\theta_2 & -\sin\theta_2 & 0 & \mathrm{L}_2\cos\theta_2\\ 0 & 0 & 0 & 1\end{bmatrix} \tag{7}
$$

$$
\begin{aligned}
&\begin{bmatrix}\frac{\mathrm{m}_1\mathrm{L}_1^2}{4}+\mathrm{I}_{zz_1}+\mathrm{m}_2\left(\frac{\mathrm{L}_2^2\sin^2\theta_2}{4}+\mathrm{L}_1{}^2\right) & -\left(\frac{\mathrm{L}_1\mathrm{L}_2\mathrm{m}_2\cos\theta_2}{2}\right)\\ -\left(\frac{\mathrm{L}_1\mathrm{L}_2\mathrm{m}_2\cos\theta_2}{2}\right) & \left(\frac{\mathrm{L}_2^2\mathrm{m}_2}{4}+\mathrm{I}_{zz_2}\right)\end{bmatrix}\begin{bmatrix}\ddot{\theta}_1\\ \ddot{\theta}_2\end{bmatrix}\\
&+\begin{bmatrix}\frac{1}{2}\left(\mathrm{L}_1\mathrm{L}_2\mathrm{m}_2\dot{\theta}_2{}^2\sin(\theta_2)\right)+\frac{1}{4}\left(\mathrm{L}_2^2\mathrm{m}_2\dot{\theta}_1\dot{\theta}_2\sin(2\theta_2)\right)\\ -\frac{1}{8}\left(\mathrm{L}_2^2\dot{\theta}_1{}^2\mathrm{m}_2\sin(2\theta_2)\right)\end{bmatrix}\\
&+\begin{bmatrix}0\\ -\frac{1}{2}\left(\mathrm{L}_2\mathrm{g}\mathrm{m}_2\sin(\theta_2)\right)\end{bmatrix}=\begin{bmatrix}\tau_1\\ 0\end{bmatrix}
\end{aligned} \tag{8}
$$

The elements of the Coriolis and Centripetal force vector are given as follows:

$$\begin{aligned}C_{11} &= I_{zz2}\dot{\theta_1}\dot{\theta_2}\sin 2\theta_2 + I_{zz3}\dot{\theta_1}\dot{\theta_2}\sin(2\theta_2+2\theta_3) \\ &+ I_{zz3}\dot{\theta_1}\dot{\theta_3}\sin(2\theta_2+2\theta_3) + a_{10}\dot{\theta_2}^2\sin\theta_2 \\ &+ \frac{a_2\dot{\theta_1}\dot{\theta_2}\sin 2\theta_2}{4} \\ &+ a_{10}\dot{\theta_2}^2\sin\theta_2 + \frac{a_2\dot{\theta_1}\dot{\theta_2}\sin 2\theta_2}{4} + a_4\dot{\theta_1}\dot{\theta_2}\sin 2\theta_2 \\ &+ \frac{a_7\dot{\theta_1}\dot{\theta_3}\sin(2\theta_2+2\theta_3)}{4} - \frac{a_{11}\dot{\theta_2}^2\sin(\theta_2+\theta_3)}{2} \\ &+ \frac{a_{11}\dot{\theta_3}^2\sin(\theta_2+\theta_3)}{2} + \frac{a_7\dot{\theta_1}\dot{\theta_2}\sin(2\theta_2+2\theta_3)}{4} \\ &+ \frac{a_9\dot{\theta_2}^2\sin\theta_2}{2} + a_{11}\dot{\theta_2}\dot{\theta_3}sin(\theta_2+\theta_3) \\ &+ a_8\dot{\theta_1}\dot{\theta_2}\sin(2\theta_2+2\theta_3) - \frac{a_8\dot{\theta_1}\dot{\theta_3}\sin\theta_3}{2} \\ &+ \frac{a_8\dot{\theta_1}\dot{\theta_3}\sin(2\theta_2+\theta_3)}{2} \end{aligned} \tag{19}$$

$$\begin{aligned}C_{21} &= \frac{-I_{zz2}\dot{\theta_1}^2\sin 2\theta_2}{2} - \frac{I_{zz3}\dot{\theta_1}^2\sin(2\theta_2+2\theta_3)}{2} \\ &- \frac{a_1\dot{\theta_1}^2\sin(2\theta_2+2\theta_3)}{8} - \frac{a_4\dot{\theta_1}^2\sin 2\theta_2}{2} \\ &- \frac{a_8\dot{\theta_3}^2\sin\theta_3}{2} - \frac{a_2\dot{\theta_1}^2\sin 2\theta_2}{8} - \frac{a_8\dot{\theta_1}^2\sin(2\theta_2+\theta_3)}{2} \\ &- a_8\dot{\theta_3}\dot{\theta_2}\sin\theta_3 \end{aligned} \tag{20}$$

$$\begin{aligned}C_{31} &= \frac{a_8\dot{\theta_1}^2\sin\theta_3}{4} - \frac{a_1\dot{\theta_1}^2\sin(2\theta_2+2\theta_3)}{8} \\ &- \frac{I_{zz3}\dot{\theta_1}^2\sin(2\theta_2+2\theta_3)}{2} + \frac{a_8\dot{\theta_2}^2\sin\theta_3}{2} \\ &- \frac{a_8\dot{\theta_1}^2\sin(2\theta_2+\theta_3)}{4} \end{aligned} \tag{21}$$

The gravity vector of the DLRIP is given in equation (22)

$$G = \begin{bmatrix} 0 \\ \dfrac{-a_{14}\sin(\theta_2+\theta_3) - a_{12}\sin\theta_2 - 2a_{13}\sin\theta_2}{2} \\ -a_{14}sin(\theta_2+\theta_3) \end{bmatrix} \tag{22}$$

The DLRIP has some complex non-linear dynamic equations which can be written in a matrix form given in equation (23):

$$\begin{bmatrix} D_{11} & D_{12} & D_{13} \\ D_{21} & D_{22} & D_{23} \\ D_{31} & D_{32} & D_{33} \end{bmatrix} \begin{bmatrix} \ddot{\theta_1} \\ \ddot{\theta_2} \\ \ddot{\theta_3} \end{bmatrix} + \begin{bmatrix} C_{11} \\ C_{21} \\ C_{31} \end{bmatrix} + \begin{bmatrix} 0 \\ G_{21} \\ G_{31} \end{bmatrix} = \begin{bmatrix} \tau_1 \\ 0 \\ 0 \end{bmatrix} \tag{23}$$

C. MODELING OF THE TLRIP

The TLRIP is assumed to be a serial kinematic chain, it is the extension of TLRIP. DH Parameters of the TLRIP are given in Table 4. The homogeneous transformation matrix of the TLRIP is derived in equation (24). Simplified parameters description of the DLRIP are given in Table 6, see appendix.

$${}^0_5T = {}^0_1T^1_2T^2_3T$$

$${}^0_5T = \begin{bmatrix} \frac{1}{2}S_{1234} + \frac{1}{2}S_{2134} & \frac{1}{2}C_{1234} + \frac{1}{2}C_{2134} & -S_1 & P_x \\ \frac{1}{2}C_{2134} - \frac{1}{2}C_{1234} & \frac{1}{2}S_{1234} - \frac{1}{2}S_{2134} & C\theta_1 & P_y \\ C_{234} & -S_{234} & 0 & P_y \\ 0 & 0 & 0 & 1 \end{bmatrix} \tag{24}$$

$$\begin{aligned}P_x &= C_1S_2(L_2 + L_3C_3 + L_4C_3C_4 - L_4S_3S_4) \\ &+ C_1C_2(L_3S_3 + L_4C_3S_4 + L_4C_4S_3) - L_1S_1 \end{aligned} \tag{25}$$

$$\begin{aligned}P_y &= S_1S_2(L_2 + L_3C_3 + L_4C_3C_4 - L_4S_3S_4) \\ &+ S_1C_2(L_3S_3 + L_4C_3S_4 + L_4C_4S_3) \end{aligned} \tag{26}$$

$$P_z = L_3C_{23} + L_2C_2 + L_4C_{234} \tag{27}$$

where $S_1 = \sin\theta_1$, $C_1 = \cos\theta_1$, $S_2 = \sin\theta_2$, $C_2 = \cos\theta_2$, $S_3 = \sin\theta_3$, $C_3 = \cos\theta_3$, $S\theta_4 = \sin\theta_4$, $C\theta_4 = \cos\theta_4$, $S_{234} = \sin(\theta_2+\theta_3+\theta_4)$, $C_{234} = \cos(\theta_2+\theta_3+\theta_4)$, $S_{1234} = \sin(\theta_1+\theta_2+\theta_3+\theta_4)$, $C_{1234} = \cos(\theta_1+\theta_2+\theta_3+\theta_4)$, $C_{2134} = \cos(\theta_2-\theta_1+\theta_3+\theta_4)$ and $S_{2134} = \sin(\theta_2-\theta_1+\theta_3+\theta_4)$.

The expression of the mass matrix of the TLRIP is given in equation (41).

$$D(\theta) = \begin{bmatrix} D_{11} & D_{12} & D_{13} & D_{14} \\ D_{21} & D_{22} & D_{23} & D_{24} \\ D_{31} & D_{32} & D_{33} & D_{34} \\ D_{41} & D_{42} & D_{43} & D_{44} \end{bmatrix} \tag{28}$$

The elements of the mass matrix of the TLRIP system are given as follows:

$$\begin{aligned}D_{11} &= \frac{a_3}{4} + I_{zz_1} + \frac{a_2\sin^2\theta_2}{4} + a_5 + \frac{I_{zz3}}{2} + a_6 + \frac{a_4}{2} + \frac{a_7}{8} \\ &- \frac{I_{zz3}\cos(2\theta_2+2\theta_3)}{2} - \frac{a_4\cos(2\theta_2)}{2} \\ &- \frac{a_7\cos(2\theta_2+2\theta_3)}{8} + \frac{a_8\cos(\theta_3)}{2} \\ &- \frac{a_8\cos(2\theta_2+\theta_3)}{2} - \frac{I_{zz4}\cos(2\theta_2+2\theta_3+2\theta_4)}{2} \\ &- \frac{a_{19}\cos(2\theta_2+2\theta_3+2\theta_4)}{8} - \frac{a_{17}\cos(2\theta_2)}{2} \\ &+ \frac{I_{zz4}}{2} + \frac{a_{17}}{2} + a_{16} + \frac{a_{18}}{2} \\ &+ \frac{a_{19}}{8} - \frac{a_{18}\cos(2\theta_2+2\theta_3)}{2} + a_{20}\cos(\theta_3) \\ &+ \frac{a_{22}\cos(\theta_4)}{2} - a_{20}\cos(2\theta_2+\theta_3) \end{aligned} \tag{29}$$

$$\begin{aligned}D_{12} &= \frac{-2a_{23}\cos(\theta_3+\theta_4) - 2a_{24}\cos\theta_2 - a_{25}\cos(\theta_2+\theta_3+\theta_4)}{2} \\ &- \frac{a_{11}\cos(\theta_2+\theta_3) + 2a_{10}\cos\theta_2}{2} - \frac{a_9\cos\theta_2}{2} \end{aligned} \tag{30}$$

$$D_{13} = -\frac{a_{11}\cos(\theta_2+\theta_3)}{2} + \frac{-2a_{23}\cos(\theta_2+\theta_3) - a_{25}\cos(\theta_2+\theta_3+\theta_4)}{2} \tag{31}$$

$$D_{14} = \frac{-a_{25}\cos(\theta_2+\theta_3+\theta_4)}{2} \tag{32}$$

$$D_{22} = \frac{a_2}{4} + I_{zz_2} + a_4 + a_8\cos\theta_3 + \frac{a_1}{4} + I_{zz3} + a_{17} + 2a_{20}\cos\theta_3 + a_{18} + \frac{a_{19}}{4} + I_{zz4} + a_{21}\cos(\theta_3+\theta_4) + a_{22}\cos\theta_4 \tag{33}$$

$$D_{23} = a_{18} + a_{22}\cos\theta_4 + a_{20}\cos\theta_3 + \frac{a_{19}}{4} + \frac{a_{21}\cos(\theta_3+\theta_4)}{2} + I_{zz4} + \frac{a_1}{4} + \frac{a_8\cos\theta_3}{2} + I_{zz3}(34) \tag{34}$$

$$D_{24} = I_{zz4} + \frac{a_{19}}{4} + \frac{a_{22}\cos\theta_4}{2} + \frac{a_{21}\cos(\theta_3+\theta_4)}{2} \tag{35}$$

$$D_{33} = \frac{a_7}{4} + I_{zz3} + I_{zz4} + a_{18} + \frac{a_{22}\cos\theta_4}{2} + \frac{a_{19}}{2} + I_{zz4} + a_{19} + \frac{a_{22}\cos\theta_4}{2} \tag{36}$$

$$D_{44} = I_{zz4} + \frac{a_{19}}{2} \tag{37}$$

$$D_{21} = D_{12}, \quad D_{31} = D_{13}, D_{41} = D_{14} \tag{38}$$

$$D_{42} = D_{24}, \quad D_{43} = D_{34} \tag{39}$$

The Coriolis and Centripetal force vector of the TLRIP can be given in equation (40).

$$C(\theta,\dot{\theta}) = \begin{bmatrix} C_{11} \\ C_{21} \\ C_{31} \\ C_{41} \end{bmatrix} \tag{40}$$

The elements of the Coriolis and Centripetal force vector of the TLRIP are given as follows:

$$\begin{aligned} C_{11} = {} & I_{zz4}\dot{\theta}_1\dot{\theta}_3\sin(2\theta_2+2\theta_3+2\theta_4) - \frac{a_8\dot{\theta}_1\dot{\theta}_3\sin\theta_3}{2} \\ & + I_{zz4}\dot{\theta}_1\dot{\theta}_2\sin(2\theta_2+2\theta_3+2\theta_4) + \frac{a_9\dot{\theta}_2^{\,2}\sin\theta_2}{2} \\ & + I_{zz4}\dot{\theta}_1\dot{\theta}_4\sin(2\theta_2+2\theta_3+2\theta_4) + I_{zz2}\dot{\theta}_1\dot{\theta}_2\sin 2\theta_2 \\ & + a_{25}\dot{\theta}_3\dot{\theta}_4\sin(\theta_3+\theta_3+\theta_4) - \frac{a_{22}\dot{\theta}_1\dot{\theta}_4\sin\theta_4}{2} \\ & + I_{zz3}\dot{\theta}_1\dot{\theta}_3\sin(2\theta_2+2\theta_3) \\ & + \frac{a_{19}\dot{\theta}_1\dot{\theta}_2\sin(2\theta_2+2\theta_3+2\theta_4)}{4} \\ & + \frac{a_{25}\dot{\theta}_2^{\,2}\sin(\theta_2+\theta_3+\theta_4)}{2} + \frac{a_{25}\dot{\theta}_3^{\,2}\sin(\theta_2+\theta_3+\theta_4)}{2} \\ & + a_8\dot{\theta}_1\dot{\theta}_2\sin(2\theta_2+\theta_3) + 2a_{23}\dot{\theta}_2\dot{\theta}_3\sin(\theta_2+\theta_3) + a_{10} \\ & + \frac{a_{21}\dot{\theta}_1\dot{\theta}_4\sin(2\theta_2+\theta_3+\theta_4)}{2} + a_{11}\dot{\theta}_2\dot{\theta}_3\sin(\theta_2+\theta_3) \\ & - \frac{a_{21}\dot{\theta}_1\dot{\theta}_3\sin(\theta_2+\theta_3)}{2} - \frac{a_{21}\dot{\theta}_1\dot{\theta}_4\sin(\theta_3+\theta_4)}{2} \\ & + a_{20}\dot{\theta}_1\dot{\theta}_3\sin(2\theta_2+\theta_3) + a_{21}\dot{\theta}_1\dot{\theta}_2\sin(2\theta_2+\theta_3+\theta_4) \\ & + \frac{a_7\dot{\theta}_1\dot{\theta}_3\sin(2\theta_2+2\theta_3)}{4} + a_{18}\dot{\theta}_1\dot{\theta}_3\sin(2\theta_2+2\theta_3) \\ & + \frac{a_{11}\dot{\theta}_2^{\,2}\sin(2\theta_2+2\theta_3)}{2} + \frac{a_8\dot{\theta}_1\dot{\theta}_3\sin(2\theta_2+\theta_3)}{2} \\ & a_8\dot{\theta}_1\dot{\theta}_2\sin(2\theta_2+\theta_3) + 2a_{20}\dot{\theta}_1\dot{\theta}_2\sin(2\theta_2+\theta_3) \\ & + a_{18}\dot{\theta}_1\dot{\theta}_2\sin(2\theta_2+2\theta_3) + a_{25}\dot{\theta}_2\dot{\theta}_4\sin(\theta_3+\theta_3+\theta_4) \\ & + 2a_{20}\dot{\theta}_1\dot{\theta}_2\sin(2\theta_2+\theta_3) \\ & - a_{20}\dot{\theta}_1\dot{\theta}_3\sin\theta_3 - \frac{a_{22}\dot{\theta}_1\dot{\theta}_3\sin\theta_4}{2} \\ & + \frac{a_{25}\dot{\theta}_4^{\,2}\sin(\theta_2+\theta_3+\theta_4)}{2} + \frac{a_{11}\dot{\theta}_3^{\,2}\sin(\theta_2+\theta_3)}{2} \\ & + a_{23}\dot{\theta}_3^{\,2}\sin(\theta_2+\theta_3)\dot{\theta}_2^{\,2}\sin\theta_2 + a_{21}\dot{\theta}_2^{\,2}\sin\theta_2 \\ & + \frac{a_{21}\dot{\theta}_1\dot{\theta}_3\sin(2\theta_2+\theta_3+\theta_4)}{2} + \frac{a_2\dot{\theta}_1\dot{\theta}_4\sin 2\theta_2}{4} \\ & + \frac{a_{19}\dot{\theta}_1\dot{\theta}_3\sin(2\theta_2+2\theta_3+2\theta_4)}{4} + a_{23}\dot{\theta}_2^{\,2}\sin(\theta_2+\theta_3) \\ & + \frac{a_{19}\dot{\theta}_1\dot{\theta}_4\sin(2\theta_2+2\theta_3+2\theta_4)}{4} \\ & + I_{zz3}\dot{\theta}_1\dot{\theta}_2\sin(2\theta_2+2\theta_3) \\ & + \frac{a_{22}\dot{\theta}_1\dot{\theta}_2\sin(2\theta_3+2\theta_3+\theta_4)}{2} + a_4\dot{\theta}_1\dot{\theta}_2\sin 2\theta_2 \\ & + \frac{a_{22}\dot{\theta}_1\dot{\theta}_3\sin(2\theta_3+2\theta_3+\theta_4)}{2} \\ & + \frac{a_1\dot{\theta}_1\dot{\theta}_2\sin(2\theta_2+2\theta_3)}{4} \\ & + a_{25}\dot{\theta}_2\dot{\theta}_3\sin(2\theta_3+2\theta_3+\theta_4) + a_{17}\dot{\theta}_1\dot{\theta}_2\sin 2\theta_2 \end{aligned} \tag{41}$$

$$\begin{aligned} C_{21} = {} & \frac{-I_{zz4}\dot{\theta}_1^{\,2}\sin(2\theta_2+2\theta_3+2\theta_4)}{2} - \frac{I_{zz2}\dot{\theta}_1^{\,2}\sin 2\theta_2}{2} \\ & - \frac{a_{17}\dot{\theta}_1^{\,2}\sin 2\theta_2}{2} - \frac{a_1\dot{\theta}_1^{\,2}\sin(2\theta_2+2\theta_3)}{8} \\ & - \frac{a_{18}\dot{\theta}_1^{\,2}\sin(2\theta_2+2\theta_3)}{2} - \frac{a_{21}\dot{\theta}_1^{\,2}\sin(2\theta_2+2\theta_3)}{2} \\ & - \frac{a_{21}\dot{\theta}_3^{\,2}\sin(\theta_3+\theta_4)}{2} - \frac{a_{21}\dot{\theta}_4^{\,2}\sin(\theta_3+\theta_4)}{2} \\ & - \frac{a_{22}\dot{\theta}_1^{\,2}\sin(2\theta_2+2\theta_3+\theta_4)}{2} - a_{21}\dot{\theta}_4\dot{\theta}_3\sin(\theta_3+\theta_4) \\ & - a_8\dot{\theta}_2\dot{\theta}_3\sin\theta_3 - 2a_{20}\dot{\theta}_2\dot{\theta}_3\sin\theta_3 - a_{22}\dot{\theta}_2\dot{\theta}_4\sin\theta_4 \\ & - \frac{a_8\dot{\theta}_3^{\,2}\sin\theta_3}{2} - a_{20}\dot{\theta}_3^{\,2}\sin\theta_3 - \frac{a_{22}\dot{\theta}_4^{\,2}\sin\theta_4}{2} \\ & - \frac{a_8\dot{\theta}_1^{\,2}\sin(2\theta_2+\theta_3)}{2} - a_{20}\dot{\theta}_1^{\,2}\sin(2\theta_2+\theta_3) \\ & - a_{20}\dot{\theta}_2\dot{\theta}_3\sin(\theta_3+\theta_4) \\ & - \frac{a_{19}\dot{\theta}_1^{\,2}\sin(2\theta_2+2\theta_3+2\theta_4)}{8} - \frac{a_4\dot{\theta}_1^{\,2}\sin 2\theta_2}{2} \\ & - a_{21}\dot{\theta}_4\dot{\theta}_2\sin(\theta_3+\theta_4) - \frac{a_2\dot{\theta}_1^{\,2}\sin 2\theta_2}{8} \\ & - \frac{I_{zz3}\dot{\theta}_1^{\,2}\sin(2\theta_2+2\theta_3)}{2} - a_{22}\dot{\theta}_3\dot{\theta}_4\sin\theta_4 \end{aligned} \tag{42}$$

$$
\begin{aligned}
C_{31} = {} & \frac{a_{21}\dot{\theta_1}^2 \sin(\theta_3+\theta_4)}{4} - \frac{I_{zz3}\dot{\theta_1}^2 \sin(2\theta_2+2\theta_3)}{2} \\
& - \frac{a_{22}\dot{\theta_4}^2 \sin\theta_4}{2} - \frac{a_1\dot{\theta_1}^2 \sin(2\theta_2+2\theta_3)}{8} \\
& - \frac{a_{18}\dot{\theta_1}^2 \sin(2\theta_2+2\theta_3)}{2} - \frac{a_{21}\dot{\theta_1}^2 \sin(2\theta_2+\theta_3+\theta_4)}{2} \\
& - \frac{I_{zz4}\dot{\theta_1}^2 \sin(2\theta_2+2\theta_3+2\theta_4)}{2} + \frac{a_{21}\dot{\theta_1}^2 \sin(\theta_2+\theta_4)}{2} \\
& + \frac{a_{20}\dot{\theta_2}^2 \sin\theta_3}{2} - \frac{a_8\dot{\theta_1}^2 \sin(2\theta_2+\theta_4)}{4} \\
& - \frac{a_{20}\dot{\theta_1}^2 \sin(2\theta_2+\theta_3)}{2} + \frac{a_{20}\dot{\theta_1}^2 \sin\theta_3}{2} \\
& - a_{22}\dot{\theta_2}\dot{\theta_4} \sin(2\theta_2+\theta_3) \\
& - \frac{a_{19}\dot{\theta_1}^2 \sin(2\theta_2+2\theta_3+2\theta_4)}{8} \\
& - \frac{a_{22}\dot{\theta_1}^2 \sin(2\theta_2+2\theta_3+2\theta_4)}{2} + \frac{a_8\dot{\theta_1}^2 \sin\theta_3}{4} \\
& + \frac{a_8\dot{\theta_2}^2 \sin\theta_3}{2} - a_{22}\dot{\theta_3}\dot{\theta_4} \sin\theta_4 \qquad (43)
\end{aligned}
$$

$$
\begin{aligned}
C_{41} = {} & \frac{a_{21}\dot{\theta_1}^2 \sin(\theta_3+\theta_4)}{4} - \frac{a_{19}\dot{\theta_1}^2 \sin(2\theta_2+2\theta_3+2\theta_4)}{8} \\
& - \frac{a_{21}\dot{\theta_1}^2 \sin(2\theta_2+\theta_3+\theta_4)}{4} \\
& - \frac{a_{22}\dot{\theta_1}^2 \sin(2\theta_2+2\theta_3+2\theta_4)}{4} \\
& - \frac{I_{zz4}\dot{\theta_1}^2 \sin(2\theta_2+2\theta_3+2\theta_4)}{2} \\
& + \frac{a_{21}\dot{\theta_2}^2 \sin(\theta_3+\theta_4)}{2} \\
& + a_{22}\dot{\theta_3}\dot{\theta_2} \sin\theta_4 + \frac{a_{22}\dot{\theta_1}^2 \sin\theta_4}{4} + \frac{a_{22}\dot{\theta_2}^2 \sin\theta_4}{2} \\
& + \frac{a_{22}\dot{\theta_3}^2 \sin\theta_4}{2} \qquad (44)
\end{aligned}
$$

The elements of the gravity vector are given as follows:

$$G_{11} = 0 \qquad (45)$$

$$
\begin{aligned}
G_{21} = {} & -\frac{a_{14}}{2}\sin(\theta_2+\theta_3) - a_{26}\sin(\theta_2+\theta_3) - \frac{a_{12}}{2}\sin\theta_2 \\
& - a_{13}\sin\theta_2 - a_{29}\sin\theta_2 - \frac{a_{27}\sin(\theta_2+\theta_3+\theta_4)}{2}
\end{aligned} \qquad (46)
$$

$$
\begin{aligned}
G_{31} = {} & -\frac{a_{27}\sin(\theta_2+\theta_3+\theta_4)}{2} - \frac{a_{14}\sin(\theta_2+\theta_3)}{2} \\
& - a_{28}\sin(\theta_2+\theta_3)
\end{aligned} \qquad (47)
$$

$$G_{41} = -\frac{a_{27}\sin(\theta_2+\theta_3+\theta_4)}{2} \qquad (48)$$

The gravity vector of the TLRIP is given in equation (49):

$$G = \begin{bmatrix} 0 \\ G_{21} \\ G_{31} \\ G_{41} \end{bmatrix} \qquad (49)$$

TABLE 4. DH-parameters of the TLRIP.

Coordinate	A_{i-1}	a_{i-1}	d_i	θ_i
1	0	0	0	θ_1
2	$-\frac{\pi}{2}$	0	L_1	$\theta_2 - \frac{\pi}{2}$
3	0	L_2	0	θ_3
4	0	L_3	0	θ_4
4	0	L_4	0	0

The TLRIP has some complex non-linear dynamic equations which can be written in a matrix form given in equation (50):

$$
\begin{bmatrix} D_{11} & D_{12} & D_{13} & D_{14} \\ D_{21} & D_{22} & D_{23} & D_{24} \\ D_{31} & D_{32} & D_{33} & D_{34} \\ D_{41} & D_{42} & D_{43} & D_{44} \end{bmatrix} \begin{bmatrix} \ddot{\theta_1} \\ \ddot{\theta_2} \\ \ddot{\theta_3} \\ \ddot{\theta_4} \end{bmatrix} + \begin{bmatrix} C_{11} \\ C_{21} \\ C_{31} \\ C_{41} \end{bmatrix} + \begin{bmatrix} 0 \\ G_{21} \\ G_{31} \\ G_{41} \end{bmatrix} = \begin{bmatrix} \tau_1 \\ 0 \\ 0 \\ 0 \end{bmatrix} \qquad (50)
$$

D. INERTIA ANALYSIS OF THE IPS

To analyze the inertia effects of the pendulums in the IPS, the nonlinear equations of the TLRIP are solved in three inertia cases. In the first analysis, the inertia tensor of all pendulums is ignored from the mathematical model. In the second analysis, the component I_{zz} of the inertia tensor is considered for mathematical modeling. In the last analysis, the full inertia tensor ${}^{i}_{i}I$ of all pendulums is taken for mathematical modeling. Figure 22 shows an example of the joints' positions of the TLRIP obtained by the three different dynamic simulation models for the initial condition of $\theta_1 = 0°$, $\theta_2 = 20°$, $\theta_3 = 30°$ and $\theta_4 = 40°$. The simulation results with only the component I_{zz} of the inertia tensor and the full inertia tensor ${}^{i}_{i}I$ are practically the same for low velocities of the pendulum. Alternatively, the nonlinear model without inertia is unacceptable. Consequently, the component Izz of the inertia tensor may be used to have a simplified nonlinear model of the IPS. Besides, the accurate nonlinear model in the swing-up control of the IPS is very important to compute the total energy of the pendulum. Therefore, the full inertia tensor ${}^{i}_{i}I$ must be taken to determine the dynamic model of the IPS.

IV. INVERTED PENDULUM SYSTEM IN CONTROL EDUCATION

According to the literature reviews, there are two balance points for the IPS. The unstable equilibrium point is where the pendulum is in an upward position and will tend to fall down unless controlled. The stable equilibrium point is where the pendulum is in a downward position and is stable without any control. Figure 23 shows an example of the stable

and unstable equilibrium points of a DLLIP. There are three main control problems related to IPS: stability, swing-up, and anti-swing. Each problem requires a different control method, which can vary depending on the model of IPS being used. The control methods applied to IPS can be classified in different ways as shown in Figure 24. For the swing-up control problem, the control methods used are: Reinforcement learning, energy-based control, adaptive control, and Lyapunov-based control methods. These methods are used to help the pendulums to reach the upward position from the downward position in a stable manner. The stability control problem considers the control of the system once it is already in the upward position. The pendulum links are held in the upward position and stationery by the experimenters while the controller is initialized. For the anti-swing control problem, the control methods used are: Feedforward control, feedback control, and impedance control methods. These methods help in reducing the oscillation and vibrations of the pendulum links during their transition from the upward to the downward position. It is worth mentioning that the choice of the control method depends on the model of IPS, the desired level of performance, and the requirement of the specific application.

A. STABILIZATION CONTROL PROBLEM

According to the works existing in the literature, it can be seen that the control methods used for the stabilization problem are: PID, optimal control, Fuzzy logic sliding mode control methods, etc. These methods are the basic methods used for the stabilization control problem of the IPS.

In 1995, Block et al. [71], mounted two pendulum links in a fixed place, and only the first pendulum link was driven by a torque motor. It is a concept of two links underactuated planar revolute robot (Pendubot). The stability of the Pendubot was achieved by linearizing the equations of motion around the equilibrium point using a linear state feedback controller and the partial feedback linearization method is applied to swing up the Pendubot.

In 1996, Wang [72], developed a stable adaptive fuzzy controller for the tracking application of SLLIP. This technique is used to keep the inverted pendulum in an upward position. The adaptive fuzzy controller is created from a group of fuzzy rules. Fuzzy parameters are adjusted online according to an adaptation law to a trajectory control of the system.

In 1996, Cheng et al. [73], developed a high-accuracy FLC to stabilize a DLLIP in the upright position. In this technique, a composition coefficient is obtained by blending fuzzy control theory with optimal control theory. Thus, a high-level resolution fuzzy controller is achieved.

In 1998, Eltohamy et al. [27], developed a single-input feedback controller for a TLLIP by using a nonlinear optimization technique. The TLLIP has been successfully stabilized in the vertical upward position. According to obtained results, the linear controller doesn't look robust enough to achieve stability.

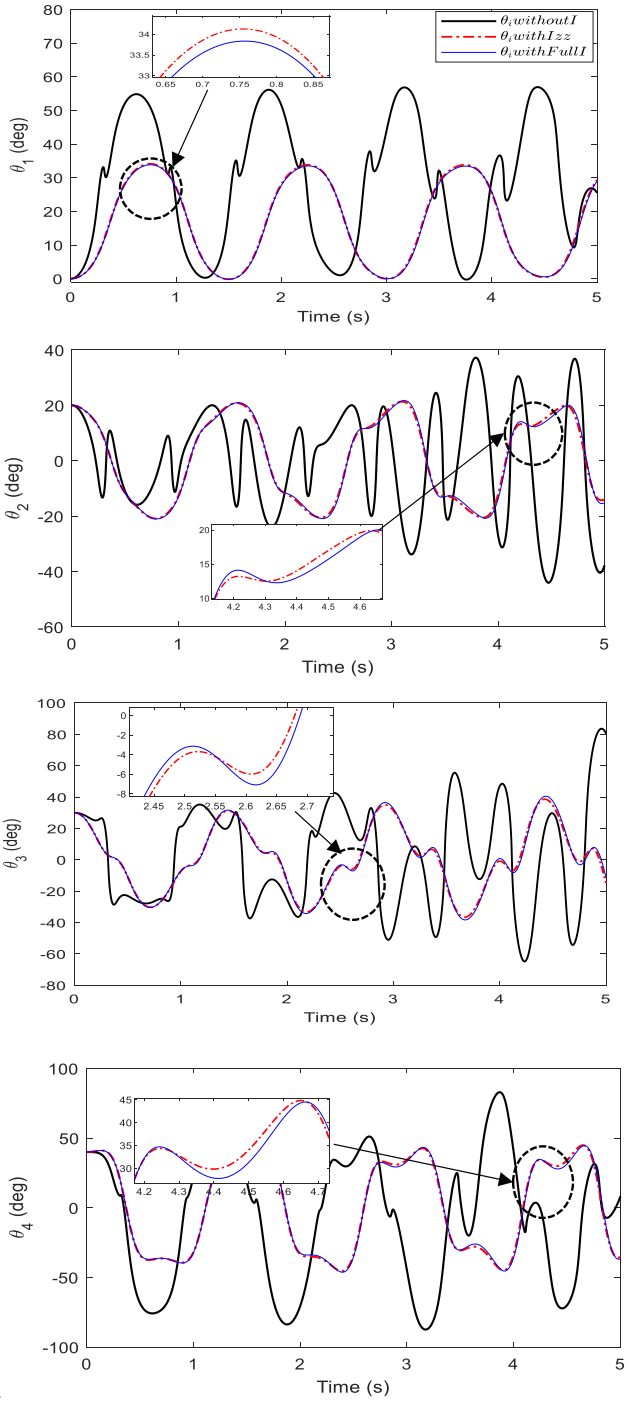

FIGURE 22. Comparison of the pendulum positions of the TLRIP in different inertia cases.

In 2000, Kim et al. [105], presented a global asymptotic stabilization method for an inverted pendulum system using an exponentially stabilizing state feedback controller. The proposed controller is designed based on the Lyapunov stability theory. The controller was applied to the global stabilization of an unstable equilibrium point of a DLLIP in the upright position.

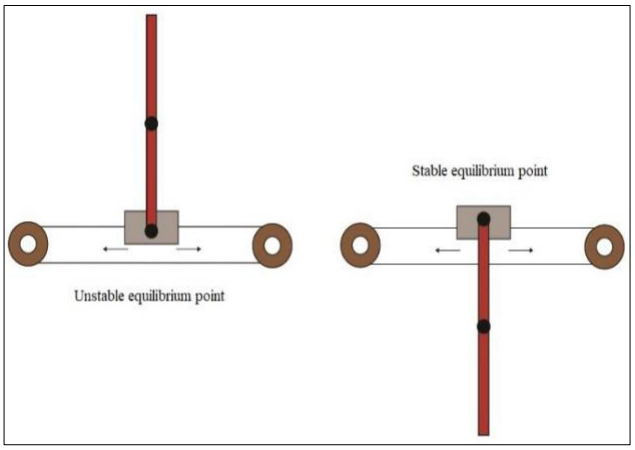

FIGURE 23. Example of the stable and unstable equilibrium points of a DLLIP.

In 2002, Aracil et al. [74], a nonlinear control law is proposed using Lyapunov theory and feedback linearization, which results in stable and robust oscillations around the vertical position of the SLRIP. The proposed technique shows improved performance compared to the traditional linear control methods.

In 2005, Feng et al. [106], proposed a fuzzy logic control method to stabilize the pendulum link in the upward position. The fuzzy logic controller is designed by using the Lyapunov stability theorem and modeling the system using a linear state-space representation. The fuzzy logic controller is used to stabilize the pendulum link by minimizing the energy of the system.

In 2010, Nasir et al. [75], developed a PID controller and Sliding Mode Control (SMC) for a SLLIP. These controllers were compared according to the time specification performance. The result indicates that SMC produced an improved response compared to the PID control strategy.

In 2010, Kizir and Bingül [76], focused on both stabilization and swing-up problems for a real experimental setup of a SLLIP. Different controllers are tested using the experimental setup. The FLC is used to swing up the pendulum. PID controller is used to stabilize the pendulum in the unstable equilibrium point.

In 2012, Zhang and Zhang [77], developed an LQR self-adjusting controller to stabilize a planar double-inverted pendulum system based on an optimized factor. The obtained results indicate that the controller ensured a fast response, good stability, and robustness in the different operating conditions applied to the system.

In 2013, Li [78], worked on the stabilization control problem of a DLRIP. An LQR based on direct adaptive fuzzy control (AFC) is developed. The AFC increases the LQR performance and the robustness of the DLRIP. The simulation results of the two controllers obtained by their comparative analysis indicate that the AFLC can enhance the LQR by increasing its robustness in the DLRIP.

In 2013, Glück et al. [31], are focused on both stabilization and swing-up problems control problems for a TLLIP. Nonlinear feedforward and optimal feedback controllers are applied for the swing-up problem. A time-variant Riccati controller was developed for system stabilization along a nominal trajectory, and an Extended Kalman Filter (EKF) was developed to estimate the no measurable states.

- In conclusion, the above research works demonstrate the various control methods that have been developed and applied for stabilizing and controlling IPS, including PID, optimal control, fuzzy logic, sliding mode control, adaptive fuzzy control, high-accuracy Fuzzy Logic Control (FLC), nonlinear optimization, and others. These control methods have been used to successfully stabilize and control the pendulum at its upright position, reduce oscillations, and improve the response of the system. The choice of control method depends on the specific requirements and objectives of each IPS system.

B. SWING-UP CONTROL PROBLEM

According to the works existing in the literature, it can be seen that the control methods used for the swing-up control problem are generally divided into, feedforward and feedback control, energy shaping, nonlinear model predictive control, and optimum trajectory approaches, etc.

Furuta et al. [79], proposed a bang-bang state feedback controller in 1992 that used the LQ control method to control the pendulum system. The controller was able to successfully swing up the pendulum to the upward position and maintain it in the unstable equilibrium point. The experimental results showed that the proposed method was robust and effective when combined with feedforward control.

In 1993, Yamakita et al. [80], proposed a method for transferring the state of a double pendulum from a stable equilibrium point to an unstable equilibrium point. This method is useful for the swing-up control problem and uses a combination of feedback and feedforward controls. The authors also employed a learning control method to adjust the feedforward control, making the overall approach a blend of both control methods.

In 1995, Yamakita et al. [81], proposed a robust approach for swinging up a DLLIP from one equilibrium to another. The authors developed two control methods for this purpose: one based on energy functions and the other based on control input, which makes the limit cycle in the system stable. The proposed approach is a significant contribution to the field of swing-up control.

In 1997, Yasunobu and Mori [82], proposed a fuzzy controller based on a formulated human control strategy and applied it to a SLLIP with unknown parameters. The swing-up control and stabilization control were modeled using Fuzzy Logic Control (FLC).

In 2000, Aström and Furuta [83], [84], studied the swing-up strategy based on the energy control method applied to a SLRIP, making a significant contribution to the field of swing-up control. These studies demonstrate the versatility of fuzzy control and its potential for solving complex control problems.

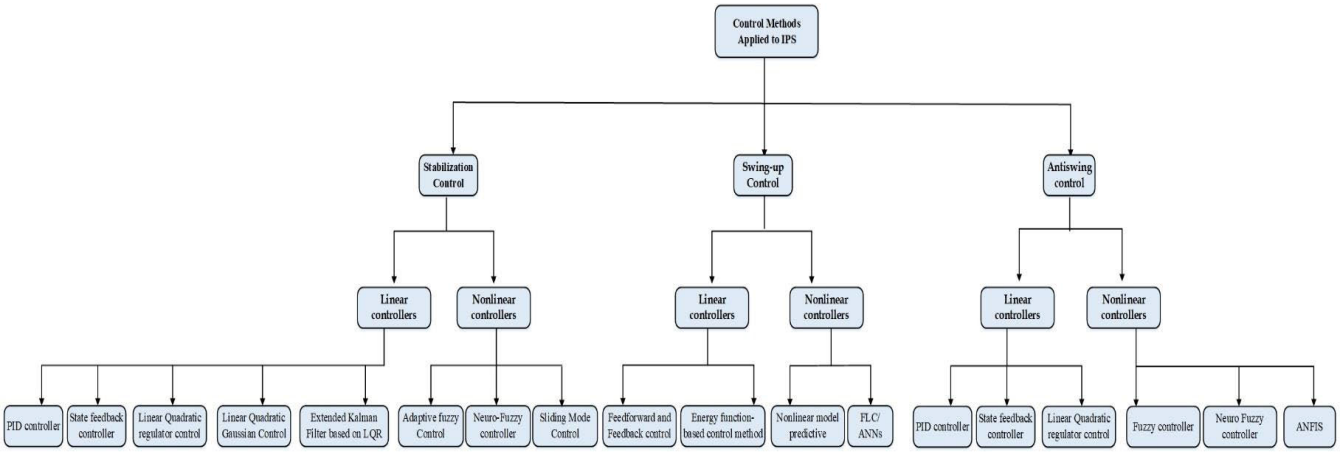

FIGURE 24. Classification of the control methods applied to IPS.

In 2002, Rubi, et al. [85], studied the swing-up problems for a DLLIP. They developed a technique to design controlled trajectories for nonlinear under-actuated mechanisms and used a linear-quadratic optimal gain scheduling controller to track the reference trajectory. This study demonstrates the effectiveness of combining optimal control with gain scheduling for solving complex control problems such as the swing-up of a DLLIP.

In 2002, Kwon [108], proposed a nonlinear optimal control method to swing up a single pendulum system by applying a combination of two different controllers. The first controller is applied to stabilize the pendulum link in the downward position, and the second controller is used to control the pendulum link from the downward position to the upward position. The nonlinear model of the pendulum system is linearized to determine the optimal control input.

In 2007, Graichen et al. [86], studied the swing-up and stability problems for a DLLIP and used a nonlinear feedforward for the swing-up problem and a linear feedback controller for the stabilization control problem.

In 2009, Wang et al. [107], proposed a fuzzy control method for the swing-up control problem of DLLIP. A fuzzy logic system was used to generate the control torque for swinging up the pendulum from the downward to the upward position. The proposed method was implemented and tested on a real pendulum system and showed promising results.

In 2014, Jaiwat and Ohtsuka [87], studied the swing-up strategies based on the nonlinear model predictive control for DLLIP.

• In summary, swing-up control is a challenging problem and there are several control methods that have been proposed in the literature to address it, including feedforward and feedback control, energy shaping, nonlinear model predictive control, and optimum trajectory approaches, among others.

C. ANTI-SWING CONTROL PROBLEM

According to the literature, nonlinear controllers are generally used for the anti-swing control problem. The nonlinear nature of the anti-swing control problem requires advanced control methods such as Nonlinear Model Predictive Control (NMPC), Feedback Linearization, and Nonlinear Feedback to ensure the desired stability and performance. These controllers can handle the complex dynamics of the system and provide robust solutions for the anti-swing control problem.

In 1998, Lee [88], proposed a dynamic model of a 3D crane system and developed an uncoupled control scheme based on the dynamic model linearized around the stable equilibrium point for the anti-swing control problem. The control scheme was designed to provide fast damping of load oscillation, precise control of crane position, and cable length with excellent transient responses for the load. The theoretical and experimental results showed the effectiveness of the proposed control scheme for solving the anti-swing control problem in 3D crane systems.

In 2000, Vikramaditya and Rajamani [89], proposed a nonlinear trajectory tracking controller for a crane system. The controller was designed using a sliding surface formulation and was demonstrated to have stability against random parameter variations and initial conditions, ensuring that it met the desired trajectory tracking specifications. The use of nonlinear control techniques, such as sliding surface control, was necessary for solving the anti-swing control problem in crane systems, as it can handle the complex dynamics and nonlinearities of the system.

In 2006, Chang et al. [90], proposed an adaptive sliding mode control approach based on fuzzy logic, applied to position control and load swing of a 3D crane system. The proposed approach involved using an adaptive slope of the sliding surface, which helped to reduce the chattering phenomenon that is often associated with sliding mode control. By incorporating fuzzy logic, the control system was able to improve its performance and handle the complex dynamics and uncertainties present in the crane system, making it a suitable solution for the anti-swing control problem.

In 2010, Solihin et al. [91], developed a Fuzzy-tuned PID controller for a robust anti-swing controller applied to a crane system. The proposed method utilizes a fuzzy system as

PID gain tuners to attain robust performance to parameters' variations for the gantry crane.

In 2013, Sun et al. [109], proposed a new method for the anti-swing control problem of the IPS. This method combined the backstepping design and the sliding mode control technique. The obtained results indicate that the proposed method effectively reduced the swing angle and improved the stability of the pendulum system in comparison to the traditional anti-swing control methods.

In 2015, Li and Li [110], proposed a hybrid control strategy combining a linear quadratic regulator and a model-based adaptive controller to control the anti-swing of a gantry crane. The proposed method is applied to the nonlinear dynamics of the gantry crane and enhances its robustness against model uncertainty and external disturbances. The simulation results showed that the proposed hybrid control strategy outperforms the traditional linear quadratic regulator and model-based adaptive control approaches. The proposed control method aims to regulate the crane system to follow a desired trajectory while maintaining stability during the anti-swing control problem. The combination of Lyapunov-based control and finite-time control is used to improve the overall performance of the system.

In 2017, Zhang et al. [92], proposed flatness-based regulation controllers for the anti-swing of crane system. Furthermore, nonlinear feedback control and a combined application of Lyapunov-based control and finite-time control are used to facilitate the development of the control laws.

V. DIFFICULTIES AND FUTURE RESEARCH DIRECTIONS

In short, controlling an IPS system is difficult due to its nonlinearity and open-loop instability. However, it can still be used in control engineering education as a tool for students to understand the challenges of controlling nonlinear systems. A robust system is necessary and control approaches must account for friction estimation in the articulations [93], [94], [95], [96], [97]. Friction estimation is crucial in controlling an IPS system as it greatly affects the response of the system. Furthermore, friction estimation can play a significant role in improving the system's quality and dynamic. Hazem et al. developed NFFEMs to estimate joint friction coefficients in the TLRIP system and compared them with AFEMs. Their study aimed to obtain joint friction models that depend on velocities and accelerations for a large range of motion trajectory that involves sudden and large changes. They also developed fuzzy-based LQR (FLQR) and fuzzy-based LQG (FLQG) controllers for stabilization and anti-swing control problems of the DLRIP and TLRIP. Further research can be focused on improving joint friction models and their impact on system control [98], [99], [100], [101]. Some future works recommendation can be given as follows:

- Further validation of the developed joint friction models through experiments and real-world applications.
- Evolutionary algorithms can be used to tune the parameters of a neuro-fuzzy system, including the ranges of fuzzification and the rules, to improve its performance in estimating the parameters of a NFFEM.
- Additional inputs such as jerks, snaps, and crackles of the pendulums can be incorporated into the neuro-fuzzy system, and the IPS (Intelligent Pendulum System) can be controlled using the friction models suggested by the neuro-fuzzy system.
- Swing-up controllers can be developed to demonstrate the experimental performance of nonlinear control algorithms such as Feedback Linearizing Quadratic Regulator (FLQR), Feedback Linearizing Quadratic Gaussian (FLQG), and Robust Backstepping Nonlinear Feedback Linearizing Quadratic Regulator (RBNF-LQR).
- The performance of the novel non-linear controllers can be compared with other controllers in the literature to evaluate their effectiveness and demonstrate their advantages and disadvantages.
- Exploration of different control strategies for improved performance, such as reinforcement learning or model predictive control.
- Integration of the developed controllers in more complex robotic systems. Investigation of the robustness and uncertainty handling capabilities of the controllers under various operating conditions [102], [103], [104].

VI. CONCLUSION

This paper introduces the different kinematic and dynamic structures of pendulum systems frequently used in literature, examining their usage in various engineering fields. Each pendulum system is an analogy of a real physical system, providing insight into its behavior. This paper summarizes and organizes the research related to controlling pendulum systems, presenting challenging applications in robotics. The aim of this review paper is to inspire researchers and generate ideas for more efficient control approaches for various robotic systems.

APPENDIX

See Tables 5 and 6.

TABLE 5. Simplified parameters description of the DLRIP.

Parameters	Description	Parameters	Description
a_1	$L_3{}^2 m_3$	a_8	$L_2 L_3 m_3$
a_2	$L_2{}^2 m_2$	a_9	$L_1 L_2 m_2$
a_3	$L_1{}^2 m_1$	a_{10}	$L_1 L_2 m_3$
a_4	$L_2{}^2 m_3$	a_{11}	$L_1 L_3 m_3$
a_5	$L_1{}^2 m_2$	a_{12}	$L_2 g m_2$
a_6	$L_1{}^2 m_3$	a_{13}	$L_2 g m_3$
a_7	$L_3{}^2 m_3$	a_{14}	$L_3 g m_3$

TABLE 6. Simplified parameters description of the TLRIP.

Parameters	Description	Parameters	Description
a_1	$L_3{}^2m_3$	a_{16}	$L_1{}^2m_4$
a_2	$L_2{}^2m_2$	a_{17}	$L_2{}^2m_4$
a_3	$L_1{}^2m_1$	a_{18}	$L_3{}^2m_4$
a_4	$L_2{}^2m_3$	a_{19}	$L_4{}^2m_4$
a_5	$L_1{}^2m_2$	a_{20}	$L_2L_3m_4$
a_6	$L_1{}^2m_3$	a_{21}	$L_2L_4m_4$
a_7	$L_3{}^2m_3$	a_{22}	$L_3L_4m_4$
a_8	$L_2L_3m_3$	a_{23}	$L_1L_3m_4$
a_9	$L_1L_2m_2$	a_{24}	$L_1L_2m_4$
a_{10}	$L_1L_2m_3$	a_{25}	$L_1L_4m_4$
a_{11}	$L_1L_3m_3$	a_{26}	L_3gm_4
a_{12}	L_2gm_2	a_{27}	L_4gm_4
a_{13}	L_2gm_3	a_{28}	L_3gm_4
a_{14}	L_3gm_3	a_{29}	L_2gm_4

REFERENCES

[1] D. C. Richard and R. H. Bishop, *Modern Control Systems*. Boston, MA, USA: Pearson Education, 1998.
[2] O. Saleem, F. Abbas, and J. Iqbal, "Complex fractional-order LQIR for inverted-pendulum-type robotic mechanisms: Design and experimental validation," *Mathematics*, vol. 11, no. 4, p. 913, Feb. 2023.
[3] G.-R. Duan, "Substability and substabilization: Control of subfully actuated systems," *IEEE Trans. Cybern.*, early access, Feb. 23, 2023, doi: 10.1109/TCYB.2023.3242277.
[4] D. J. Ness, "Small oscillations of a stabilized, inverted pendulum," *Amer. J. Phys.*, vol. 35, no. 10, pp. 964–967, Oct. 1967.
[5] L. Blitzer, "Inverted pendulum," *Amer. J. Phys.*, vol. 33, no. 12, pp. 1076–1078, 1965.
[6] J. L. Bogdanoff and S. J. Citron, "Experiments with an inverted pendulum subject to random parametric excitation," *J. Acoust. Soc. Amer.*, vol. 38, no. 3, pp. 447–452, 1965.
[7] H. P. Kalmus, "The inverted pendulum," *Amer. J. Phys.*, vol. 38, no. 7, pp. 874–878, 1970.
[8] K. H. Lundberg, "History of inverted-pendulum systems," *IFAC Proc.*, vol. 42, no. 24, pp. 131–135, 2010.
[9] Y. Yang, H. H. Zhang, and R. M. Voyles, "Optimal fractional-order proportional–integral–derivative control enabling full actuation of decomposed rotary inverted pendulum system," *Trans. Inst. Meas. Control*, vol. 2023, Jan. 2023, Art. no. 014233122211466.
[10] R. Mondal and J. Dey, "A novel design methodology on cascaded fractional order (FO) PI-PD control and its real time implementation to cart-inverted pendulum system," *ISA Trans.*, vol. 130, pp. 565–581, Nov. 2022.
[11] S. J. Chacko and R. J. Abraham, "On LQR controller design for an inverted pendulum stabilization," *Int. J. Dyn. Control*, vol. 2022, pp. 1–9, Nov. 2022.
[12] O. Saleem and K. Mahmood-Ul-Hasan, "Indirect adaptive state-feedback control of rotary inverted pendulum using self-mutating hyperbolic-functions for online cost variation," *IEEE Access*, vol. 8, pp. 91236–91247, 2020.
[13] M. F. Hamza, H. J. Yap, I. A. Choudhury, A. I. Isa, A. Y. Zimit, and T. Kumbasar, "Current development on using rotary inverted pendulum as a benchmark for testing linear and nonlinear control algorithms," *Mech. Syst. Signal Process.*, vol. 116, pp. 347–369, Feb. 2019.
[14] Z. Ping, M. Zhou, C. Liu, Y. Huang, M. Yu, and J. G. Lu, "An improved neural network tracking control strategy for linear motor-driven inverted pendulum on a cart and experimental study," *Neural Comput. Appl.*, vol. 34, pp. 1–8, Jul. 2022.
[15] A. Mahapatro, P. R. Dhal, D. R. Parhi, M. K. Muni, C. Sahu, and S. K. Patra, "Towards stabilization and navigational analysis of humanoids in complex arena using a hybridized fuzzy embedded PID controller approach," *Expert Syst. Appl.*, vol. 213, Mar. 2023, Art. no. 119251.
[16] E. Susanto, A. S. Wibowo, and E. G. Rachman, "Fuzzy swing up control and optimal state feedback stabilization for self-erecting inverted pendulum," *IEEE Access*, vol. 8, pp. 6496–6504, 2020.
[17] U. Onen, "Model-free controller design for nonlinear underactuated systems with uncertainties and disturbances by using extended state observer based chattering-free sliding mode control," *IEEE Access*, vol. 11, pp. 2875–2885, 2023.
[18] A. Nagarajan and A. A. Victoire, "Optimization reinforced PID-sliding mode controller for rotary inverted pendulum," *IEEE Access*, vol. 11, pp. 24420–24430, 2023.
[19] S. Zeghlache, M. Z. Ghellab, A. Djerioui, B. Bouderah, and M. F. Benkhoris, "Adaptive fuzzy fast terminal sliding mode control for inverted pendulum-cart system with actuator faults," *Math. Comput. Simul.*, vol. 210, pp. 207–234, Aug. 2023.
[20] A. de Carvalho, B. A. Angelico, J. F. Justo, A. M. de Oliveira, and J. I. da Silva Filho, "Model reference control by recurrent neural network built with paraconsistent neurons for trajectory tracking of a rotary inverted pendulum," *Appl. Soft Comput.*, vol. 133, Jan. 2023, Art. no. 109927.
[21] M. Bettayeb, C. Boussalem, and R. Mansouri, "Stabilization of an inverted pendulum-cart system by fractional PI-state feedback," *ISA Trans.*, vol. 53, no. 2, pp. 508–516, 2014.
[22] A. K. Stimac, "Standup and stabilization of the inverted pendulum," Ph.D. dissertation, Massachusetts Inst. Technol., Cambridge, MA, USA, 1999.
[23] S. Krafes, Z. Chalh, and A. Saka, "A review on the control of second order underactuated mechanical systems," *Complexity*, vol. 2018, pp. 1–17, Dec. 2018.
[24] X. Chen, R. Yu, K. Huang, S. Zhen, H. Sun, and K. Shao, "Linear motor driven double inverted pendulum: A novel mechanical design as a testbed for control algorithms," *Simul. Model. Pract. Theory*, vol. 81, pp. 31–50, Feb. 2018.
[25] H. Niemann and J. K. Poulsen, "Design and analysis of controllers for a double inverted pendulum," *ISA Trans.*, vol. 44, no. 1, pp. 63–145, 2005.
[26] B. Naghmehm, A. Hooshiar, J. Masoudrazban, and C.-Y. Su, "Stabilization of double inverted pendulum on cart: LQR approach," *Int. J. Mech. Prod. Eng.*, vol. 5, p. 2, Jan. 2017.
[27] K. G. Eltohamy and C. Y. Kuo, "Nonlinear optimal control of a triple link inverted pendulum with single control input," *Int. J. Control*, vol. 69, no. 2, pp. 239–256, 1998.
[28] K. G. Eltohamy and C. Y. Kuo, "Real time stabilisation of a triple link inverted pendulum using single control input," *IEE Proc.-Control Theory Appl.*, vol. 144, no. 5, pp. 498–504, Sep. 1997.
[29] S. Sehgal and S. Tiwari, "LQR control for stabilizing triple link inverted pendulum system," in *Proc. 2nd Int. Conf. Power, Control Embedded Syst.*, Dec. 2012, pp. 1–5.
[30] V. Setka, R. Cecil, and M. Schlegel, "Triple inverted pendulum system implementation using a new ARM/FPGA control platform," in *Proc. 18th Int. Carpathian Control Conf. (ICCC)*, May 2017, pp. 321–326.
[31] T. Glück, A. Eder, and A. Kugi, "Swing-up control of a triple pendulum on a cart with experimental validation," *Automatica*, vol. 49, no. 3, pp. 801–808, 2013.
[32] E. Franco, A. Astolfi, and F. Y. Baena, "Robust balancing control of flexible inverted-pendulum systems," *Mechanism Mach. Theory*, vol. 130, pp. 539–551, Jan. 2018.
[33] P. S. Gandhi, P. Borja, and R. Ortega, "Energy shaping control of an inverted flexible pendulum fixed to a cart," *Control Eng. Pract.*, vol. 56, pp. 27–36, Nov. 2016.
[34] K. Walker and H. Hauser, "Evolving optimal learning strategies for robust locomotion in the spring-loaded inverted pendulum model," *Int. J. Adv. Robot. Syst.*, vol. 16, no. 6, Nov. 2019, Art. no. 172988141988570.
[35] U. Saranlı, Ö. Arslan, M. M. Ankarali, and Ö. Morgül, "Approximate analytic solutions to non-symmetric stance trajectories of the passive spring-loaded inverted pendulum with damping," *Nonlinear Dyn.*, vol. 62, no. 4, pp. 729–742, 2010.
[36] R. Blickhan, "The spring-mass model for running and hopping," *J. Biomech.*, vol. 22, no. 11–12, pp. 1217–1227, 1989.

[37] Q. Luo, C. Chevallereau, and Y. Aoustin, "Walking stability of a variable length inverted pendulum controlled with virtual constraints," *Int. J. Humanoid Robot.*, vol. 16, no. 6, Dec. 2019, Art. no. 1950040.

[38] D. S. D. Stilling and W. Szyszkowski, "Controlling angular oscillations through mass reconfiguration: A variable length pendulum case," *Int. J. Non-Linear Mech.*, vol. 37, no. 1, pp. 89–99, 2002.

[39] E. M. Navarro-López and E. Fossas-Colet, "Stabilization of the variable-length pendulum," in *Proc. Eur. Control Conf. (ECC)*, Sep. 2001, pp. 675–680.

[40] L. Xing, Y. Chen, and X. Wu, "A novel parallel-type double inverted pendulum control method," in *Proc. IEEE Int. Conf. Intell. Comput. Intell. Syst.*, Oct. 2010, pp. 880–887.

[41] X. Xin and M. Kaneda, "Analysis of the energy-based control for swinging up two pendulums," *IEEE Trans. Autom. Control*, vol. 50, no. 5, pp. 679–684, 2005.

[42] M. Deng, A. Inoue, T. Henmi, and N. Ueki, "Analysis and experiment on simultaneous swing? Up of a parallel cart type double inverted pendulum," *Asian J. Control*, vol. 10, no. 1, pp. 121–128, 2008.

[43] M. Akhtaruzzaman and A. A. Shafie, "Modeling and control of a rotary inverted pendulum using various methods, comparative assessment and result analysis," in *Proc. IEEE Int. Conf. Mechatronics Autom.*, Aug. 2010, pp. 1342–1347.

[44] P. Dwivedi, S. Pandey, and A. S. Junghare, "Stabilization of unstable equilibrium point of rotary inverted pendulum using fractional controller," *J. Franklin Inst.*, vol. 354, no. 17, pp. 7732–7766, Nov. 2017.

[45] M. Ramírez-Neria, H. Sira-Ramírez, R. Garrido-Moctezuma, and A. Luviano-Juarez, "Linear active disturbance rejection control of underactuated systems: The case of the Furuta pendulum," *ISA Trans.*, vol. 53, no. 4, pp. 920–928, 2014.

[46] S. Awtar, N. King, T. Allen, I. H. M. Bang, D. Skidmore, and K. Craig, "Inverted pendulum systems: Rotary and arm-driven—A mechatronic system design case study," *Mechatronics*, vol. 12, no. 2, pp. 357–370, 2002.

[47] A. Jabbar, F. M. Malik, and S. A. Sheikh, "Nonlinear stabilizing control of a rotary double inverted pendulum: A modified backstepping approach," *Trans. Inst. Meas. Control*, vol. 39, no. 11, pp. 1721–1734, 2017.

[48] S. Jadlovský and J. Sarnovský, "Modelling of classical and rotary inverted pendulum systems—A generalized approach," *J. Electr. Eng.*, vol. 64, no. 1, pp. 12–19, Jan. 2013.

[49] I. Fantoni, R. Lozano, and M. W. Spong, "Energy based control of the pendubot," *IEEE Trans. Autom. Control*, vol. 45, no. 4, pp. 725–729, Apr. 2000.

[50] M. Zhang and T.-J. Tarn, "Hybrid control of the Pendubot," *IEEE/ASME Trans. Mechatronics*, vol. 7, no. 1, pp. 79–86, Mar. 2002.

[51] R. Tedrake, "Underactuated robotics: Learning, planning, and control for efficient and agile machines," MIT, Cambridge, MA, USA, Tech. Rep., 6.832, 2009.

[52] M. W. Spong, "The swing up control problem for the acrobot," *IEEE Control Syst.*, vol. 15, no. 1, pp. 49–55, Feb. 1995.

[53] S. A. Bortoff and M. W. Spong, "Pseudolinearization of the acrobot using spline functions," in *Proc. 31st IEEE Conf. Decis. Control*, Dec. 1992, pp. 593–598.

[54] M. W. Spong, P. Corke, and R. Lozano, "Nonlinear control of the reaction wheel pendulum," *Automatica*, vol. 37, no. 11, pp. 1845–1851, 2001.

[55] O. D. Montoya and W. Gil-González, "Nonlinear analysis and control of a reaction wheel pendulum: Lyapunov-based approach," *Int. J. Eng. Sci. Technol.*, vol. 23, no. 1, pp. 21–29, 2020.

[56] B. Krishna, D. Chandran, and I. Thirunavukkarasu, "Modeling and performance comparison of triple PID and LQR controllers for parallel rotary double inverted pendulum," *Int. J. Emerg. Trends Electr. Electron.*, vol. 11, no. 2, pp. 145–150, 2015.

[57] R. Horvath, G. T. Flowers, and R. A. Overfelt, "Stability investigation of a two-link 3DOF rotational pendulum," in *Proc. 19th Biennial Conf. Mech. Vib. Noise*, Jan. 2003, pp. 903–912.

[58] L. Feng, T. Yongchuan, and Q. Qian, "Stabilize the planar single inverted pendulum based on LQR," in *Proc. IEEE Int. Conf. Autom. Logistics (ICAL)*, Aug. 2011, pp. 238–242.

[59] N. Gupta and L. Dewan, "Modeling and simulation of rotary-rotary planer inverted pendulum," *J. Phys., Conf. Ser.*, vol. 1240, no. 1, 2019, Art. no. 012089.

[60] A. Najdecka, S. Narayanan, and M. Wiercigroch, "Rotary motion of the parametric and planar pendulum under stochastic wave excitation," *Int. J. Non-Linear Mech.*, vol. 71, pp. 30–38, May 2015.

[61] S. W. Nawawi, M. N. Ahmad, and J. H. Osman, "Real-time control of a two-wheeled inverted pendulum mobile robot," *World Academy Sci., Eng. Technol.*, vol. 39, pp. 214–220, Jan. 2008.

[62] S. Jeong and T. Takahashi, "Wheeled inverted pendulum type assistant robot: Design concept and mobile control," *Intell. Service Robot.*, vol. 1, no. 4, pp. 313–320, 2008.

[63] P. Chowdhary, V. Gupta, D. Gupta, A. Jadhav, and V. Mishra, "Design of two wheel self balancing robot using PID controller," *Int. J. Eng. Res. Technol.*, vol. 5, no. 1, pp. 1–10, 2017.

[64] O. Aly, M. K. Abd-Al-Azeem, R. Mohammed, M. Aly, and S. I. Mohammed, "Balancing a two-wheeled robot," Undergraduate thesis, Dept. Comput. Syst., Minia Univ., Egypt, 2009.

[65] S. Jin and Y. Ou, "A wheeled inverted pendulum learning stable and accurate control from demonstrations," *Appl. Sci.*, vol. 9, no. 24, p. 5279, Dec. 2019.

[66] C. Zhang, H. Hu, D. Gu, and J. Wang, "Cascaded control for balancing an inverted pendulum on a flying quadrotor," *Robotica*, vol. 35, no. 6, pp. 1263–1279, 2017.

[67] M. Hehn and R. D'Andrea, "A flying inverted pendulum," in *Proc. IEEE Int. Conf. Robot. Autom.*, May 2011, pp. 763–770.

[68] S. Kucuk and Z. Bingul, "Inverse kinematics solutions for industrial robot manipulators with offset wrists," *Appl. Math. Model.*, vol. 38, no. 7, pp. 1983–1999, 2014.

[69] S. Kucuk and Z. Bingul, *Robot Kinematics: Forward and Inverse Kinematics*. London, U.K.: Intech Open, 2006.

[70] S. Kucuk and Z. Bingul, *Robot DinamiĞi ve Kontrolü*. Istanbul, Türkiye: Birsen YayÝnevi, 2008.

[71] M. W. Spong and D. J. Block, "The Pendubot: A mechatronic system for control research and education," in *Proc. 34th IEEE Conf. Decis. Control*, Dec. 1995, pp. 555–556.

[72] L. X. Wang, "Stable adaptive fuzzy controllers with application to inverted pendulum tracking," *IEEE Trans. Syst., Man, Cybern., B, Cybern.*, vol. 26, no. 5, pp. 677–691, Sep. 1996.

[73] F. Cheng, G. Zhong, Y. Li, and Z. Xu, "Fuzzy control of a double-inverted pendulum," *Fuzzy Sets Syst.*, vol. 79, no. 3, pp. 315–321, 1996.

[74] J. Aracil, F. Gordillo, and J. A. Acosta, "Stabilization of oscillations in the inverted pendulum," *IFAC Proc. Volumes*, vol. 35, no. 1, pp. 79–84, 2002.

[75] A. N. Nasir, R. M. Ismail, and M. A. Ahmad, "Performance comparison between sliding mode control (SMC) and PD-PID controllers for a nonlinear inverted pendulum system," *World Academy Sci., Eng. Technol.*, vol. 71, pp. 400–405, Jan. 2010.

[76] S. Kizir, Z. Bingül, and C. Oysu, "Fuzzy control of a real time inverted pendulum system," *J. Intell. Fuzzy Syst.*, vol. 21, no. 1, pp. 121–133, 2010.

[77] J. L. Zhang and W. Zhang, "LQR self-adjusting based control for the planar double inverted pendulum," *Phys. Proc.*, vol. 24, pp. 1669–1676, Jan. 2012.

[78] B. Li, "Rotational double inverted pendulum," M.S. thesis, Dept. Elect. Eng., Dayton, OH, USA, 2013.

[79] K. Furuta, M. Yamakita, and S. Kobayashi, "Swing-up control of inverted pendulum using pseudo-state feedback," *Proc. Inst. Mech. Eng., I, J. Syst. Control Eng.*, vol. 206, no. 4, pp. 263–269, 1992.

[80] M. Yamakita, K. Nonaka, and K. Furuta, "Swing up control of a double pendulum," in *Proc. Amer. Control Conf.*, Jun. 1993, pp. 2229–2233.

[81] M. Yamakita, M. Iwashiro, Y. Sugahara, and K. Furuta, "Robust swing up control of double pendulum," in *Proc. Amer. Control Conf.*, 1995, pp. 290–295.

[82] S. Yasunobu and M. Mori, "Swing up fuzzy controller for inverted pendulum based on a human control strategy," in *Proc. 6th Int. Fuzzy Syst. Conf.*, vol. 3, Jul. 1997, pp. 1621–1625.

[83] K. J. Åström and K. Furuta, "Swinging up a pendulum by energy control," *Automatica*, vol. 36, no. 2, pp. 287–295, 2000.

[84] K. J. Åström and K. Furuta, "Swinging up a pendulum by energy control," *IFAC Proc.*, vol. 29, no. 1, pp. 1919–1924, 1996.

[85] J. Rubı, A. Rubio, and A. Avello, "Swing-up control problem for a self-erecting double inverted pendulum," *IEE Proc.-Control Theory Appl.*, vol. 149, no. 2, pp. 169–175, 2002.

[86] K. Graichen, M. Treuer, and M. Zeitz, "Swing-up of the double pendulum on a cart by feedforward and feedback control with experimental validation," *Automatica*, vol. 43, no. 1, pp. 63–71, Jan. 2007.

[87] P. Jaiwat and T. Ohtsuka, "Real-time swing-up of double inverted pendulum by nonlinear model predictive control," in *Proc. Int. Symp. Adv. Control Ind. Processes*, 2014, pp. 290–295.
[88] H. H. Lee, "Modeling and control of a three-dimensional overhead crane," *J. Dyn. Syst. Meas. Control*, vol. 120, no. 4, pp. 471–476, 1998.
[89] B. Vikramaditya and R. Rajamani, "Nonlinear control of a trolley crane system," in *Proc. Amer. Control Conf.*, 2000, pp. 1032–1036.
[90] C. Y. Chang, "Adaptive fuzzy controller of the overhead cranes with nonlinear disturbance," *IEEE Trans. Ind. Informat.*, vol. 3, no. 2, pp. 164–172, May 2007.
[91] M. I. Solihin and L. A. Wahyudi, "Fuzzy-tuned PID anti-swing control of automatic gantry crane," *J. Vib. Control*, vol. 16, no. 1, pp. 127–145, 2010.
[92] Z. Zhang, Y. Wu, and J. Huang, "Differential-flatness-based finite-time anti-swing control of underactuated crane systems," *Nonlinear Dyn.*, vol. 87, no. 3, pp. 1749–1761, 2017.
[93] D. Park, D. Chwa, and S.-K. Hong, "An estimation and compensation of the friction in an inverted pendulum," in *Proc. SICE-ICASE Int. Joint Conf.*, 2006, pp. 779–783.
[94] L. Fang, W. Ji Chen, and S. Un Cheang, "Friction compensation for a double inverted pendulum," in *Proc. IEEE Int. Conf. Control Appl.*, Aug. 2001, pp. 908–913.
[95] M. Gafvert, J. Svensson, and K. J. Astrom, "Friction and friction compensation in the Furuta pendulum," in *Proc. Eur. Control Conf. (ECC)*, Aug. 1999, pp. 3154–3159.
[96] P. E. Dupont, "Friction modeling in dynamic robot simulation," in *Proc. Int. Conf. Robot. Autom.*, 1990, pp. 1370–1376.
[97] P. E. Dupont, "The effect of friction on the forward dynamics problem," *Int. J. Robot. Res.*, vol. 12, no. 2, pp. 164–179, 1993.
[98] Z. B. Hazem, M. J. Fotuhi, and Z. Bingül, "A comparative study of the joint neuro-fuzzy friction models for a triple link rotary inverted pendulum," *IEEE Access*, vol. 8, pp. 49066–49078, 2020.
[99] Z. B. Hazem, M. J. Fotuhi, and Z. Bingül, "A comparative study of the friction models with adaptive coefficients for a rotary triple inverted pendulum," in *Proc. 6th Int. Conf. Control Eng. Inf. Technol. (CEIT)*, 2018, pp. 1–6.
[100] M. J. Fotuhi, Z. B. Hazem, and Z. Bingul, "Comparison of joint friction estimation models for laboratory 2 DOF double dual twin rotor aerodynamical system," in *Proc. 44th Annu. Conf. IEEE Ind. Electron. Soc.*, Oct. 2018, pp. 2231–2236.
[101] M. J. Fotuhi, Z. B. Hazem, and Z. Bingül, "Adaptive joint friction estimation model for laboratory 2 DOF double dual twin rotor aerodynamical helicopter system," in *Proc. Int. Conf. Control Eng. Inf. Technol. (CEIT)*, 2018, pp. 1–6.
[102] Z. B. Hazem, M. J. Fotuhi, and Z. Bingül, "Development of a fuzzy-LQR and fuzzy-LQG stability control for a double link rotary inverted pendulum," *J. Franklin Inst.*, vol. 357, no. 15, pp. 10529–10556, Oct. 2020.
[103] Z. B. Hazem, M. J. Fotuhi, and Z. Bingül, "A study of anti-swing fuzzy LQR control of a double serial link rotary pendulum," *IETE J. Res.*, vol. 2021, pp. 1–12, Apr. 2021.
[104] Z. B. Hazem, M. J. Fotuhi, and Z. Bingül, "Anti-swing radial basis neuro-fuzzy linear quadratic regulator control of double link rotary pendulum," *Proc. Inst. Mech. Eng., I, J. Syst. Control Eng.*, vol. 236, no. 3, pp. 531–545, Mar. 2022.
[105] B.-J. Choi, S.-W. Kwak, and B. K. Kim, "Design and stability analysis of single-input fuzzy logic controller," *IEEE Trans. Syst., Man, B, Cybern.*, vol. 30, no. 2, pp. 303–309, Apr. 2000.
[106] G. Feng, C. L. Chen, D. Sun, and Y. Zhu, "H_∞ controller synthesis of fuzzy dynamic systems based on piecewise Lyapunov functions and bilinear matrix inequalities," *IEEE Trans. Fuzzy Syst.*, vol. 13, no. 1, pp. 103–194, Feb. 2005.
[107] C. Wang Tao, J. Taur, J. H. Chang, and S.-F. Su, "Adaptive fuzzy switched swing-up and sliding control for the double-pendulum-and-cart system," *IEEE Trans. Syst., Man, Cybern., B, Cybern.*, vol. 40, no. 1, pp. 241–252, Feb. 2010.
[108] Y. H. Kwon, B. S. Kim, S. Y. Lee, and M. T. Lim, "Composite control for inverted pendulum system," *Trans. Control, Automat. Syst. Eng.*, vol. 4, no. 1, pp. 84–91, 2002.
[109] N. Sun, Y. Fang, and X. Zhang, "Energy coupling output feedback control of 4-DOF underactuated cranes with saturated inputs," *Automatica*, vol. 49, no. 5, pp. 1318–1325, 2013.
[110] W. Yu and X. Li, "Anti-swing control for an overhead crane with intelligent compensation," in *Proc. 3rd Int. Symp. Resilient Control Syst.*, Aug. 2010, pp. 1–10.

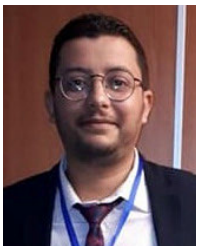

ZIED BEN HAZEM (Member, IEEE) received the bachelor's degree in mechanical engineering from the Higher Institute of Technological Studies (ISETR), Rades, Tunisia, in 2011, the master's degree (research) in automatic control, robotics, and information processing field of electronic, electrical, and automation engineering (EEA) from the Department of Electrical Engineering, National School of Engineering of Carthage (ENICarthag), Carthage University, Tunisia, in 2013, and the Ph.D. degree in mechatronics engineering from the Engineering Faculty, Kocaeli University, Turkey, in 2021. He is currently an Assistant Professor Doctor with the Mechatronics Engineering Department, University of Technology Bahrain, Bahrain. His current research interests include artificial intelligence in robot control systems, collaborative robots, open-source robotics, deep reinforcement learning for robot, deep learning models in robotics, and robotic operating systems.

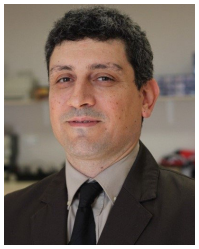

ZAFER BINGÜL (Member, IEEE) received the B.A. degree from Istanbul Technical University, Istanbul, Turkey, in 1992, and the M.S. and Ph.D. degrees from Vanderbilt University, Nashville, TN, USA, in 1996 and 2000, respectively, all in electrical engineering. From 1999 to 2000, he was a Research Associate with the Electrical Engineering Department, Tennessee State University, Nashville, where he was engaged in research and application of genetic algorithms for multiobjective optimization problems. He is currently a Professor in mechatronics engineering with the School of Engineering, Kocaeli University, Kocaeli, Turkey. His research interests include robotics and welding automation, optimization, evolutionary algorithms, and control.